DEXTRIN VESICLES AND THEIR ENCAPSULATION CAPABILITIES FOR DRUG DELIVERY

Thesis Submitted towards the Partial fulfillment of
BS-MS dual degree programme

By

UMA SRIDHAR
20081051

Under the guidance of

Dr. M. Jayakannan
Associate Professor
Department of Chemistry
IISER, Pune

भारतीय विज्ञान शिक्षा एवं अनुसंधान संस्थान, पुणे
INDIAN INSTITUTE OF SCIENCE EDUCATION AND RESEARCH (IISER) PUNE
(An Autonomous Institution of Ministry of Human Resource Development, Govt. of India)
Sai Trinity Building, Garware Circle, Pashan Pune - 411 021

Dr. M. Jayakannan
Associate Professor
Department of Chemistry

CERTIFICATE

This is to certify that this dissertation entitled "**Dextrin vesicles and their encapsulation capabilities for drug delivery**" towards the partial fulfilment of the BS-MS dual degree programme at the Indian Institute of Science Education and Research, Pune represents original research carried out by Uma Sridhar, IISER, Pune under my supervision at IISER, Pune during the academic year 2011-2012.

Date:

Place: Signature

DECLARATION

I hereby declare that the matter embodied in the report entitled "**Dextrin vesicles and their encapsulation capabilities for drug delivery** " are the results of the investigations carried out by me at the Department of Chemistry, IISER, Pune, under the supervision of Dr. M. Jayakannan and the same has not been submitted elsewhere for any other degree.

Date:

Place: Signature

ACKNOWLEDGEMENT

It is a pleasure to thank those who made this thesis possible. First and foremost, I would like to thank my advisor **Dr. M. Jayakannan** for his immense support and guidance. I feel privileged to be among his students. He celebrates research in the truest sense of the term. I would also like to thank him for providing us with such an excellent opportunity, and also for his encouragement throughout the duration of the project. Despite his busy schedule, he always found time to discuss with us and guide us throughout the project. His guidance has been an extraordinary learning experience.

I would like to express my sincere gratitude to ***Prof. K.N. Ganesh,*** Director IISER-Pune for the state-of-the-art amenities and instrumentation in IISER, Pune.

I would like to thank **Pramod and Smita** who mentored me during the course of the project. They provided me with the insight, constant help throughout the project and answered all my questions patiently.

I thank all my lab mates Bala, Mahima, Shekhar, Anantharaj, Moumita, Rajendra, Narasimha and Bhagyashree for making the memories in Mendeleev Block fond and special. This place has left a lasting impression in me. This has been undoubtedly the best environment I have studied in and the above people were responsible for it.

Last but not the least; I owe my deep sense of gratitude to my family and friends as they have been very supportive throughout my life during the good and hard times.

-Uma

CONTENTS

ABSTRACT

This thesis emphasizes a facile method of preparing dextrin (starch derivative) amphiphiles using renewable hydrophobic units such as 3-pentadecylphenol as the hydrophobic moiety. Dextrin amphiphiles with different degree of substitutions were synthesized and their structures were characterized by NMR and FTIR techniques. The self assembly of the newly synthesized amphiphiles were investigated using dynamic light scattering, electron microscope (SEM and TEM) and atomic force microscopic techniques. The critical vesicular concentrations (CVCs) were determined using pyrene as fluorophore. Further, the encapsulation capabilities of the dextrin scaffolds were investigated using hydrophobic and hydrophilic dye molecules. The results proved that dextrin with 7 % hydrophobic substitution stabilizes the Rhodamine-B (Rh-B) in the vesicular scaffold. On the other hand, higher incorporation of hydrophobic content fails to show any encapsulation. The in-vitro release characteristics of Rhodamine-B loaded dextrin vesicles were studied under physiological conditions. Esterase enzyme was employed as stimuli to breakdown he vesicular scaffolds and delivers the encapsulated cargo at much faster rate. The study gives an insight into role of the hydrophobic unit in the self assembly and the forces that are responsible for giving rise to these structures at the molecular level. The scaffolds, thus synthesized could be used for the loading and delivery of hydrophobic as well as hydrophilic anticancer drugs which are currently investigated in detail.

INTRODUCTION

1.1 INTRODUCTION

Drug delivery is the method or process of administering a pharmaceutical compound to achieve a therapeutic effect in humans or animals. [1] Conventional drug delivery systems including capsules, ointment, creams, lotions, injections etc. have drawbacks such as rapid blood clearance due to opsonisation by plasma proteins, dose variation and severe side effects due to lack of selectivity.[2] The need to maintain in blood is one of the main goals in therapeutic and diagnostic applications, which are often hampered by the short in vivo half-life of administered compounds. Many factors are involved in the removal of substances from the circulation: proteins and peptides are rapidly eliminated by proteolytic degradation, renal filtration, and/or immunogenic and antigenic reactions.[3] Drug molecules that show a therapeutic window phenomenon where, the concentration above which the drug is toxic and below which its action is inefficient cannot be administered using conventional delivery systems because frequent dosage of drugs results in sudden changes between the toxic and required levels. Controlled release systems aim to improve the efficacy of the drug by delivering the drug over an extended duration or at a specific time during treatment ensuring very small fluctuations in the drug concentration.[4] Controlled release over an extended duration is highly beneficial for drugs that are rapidly metabolized and eliminated from the body after administration.

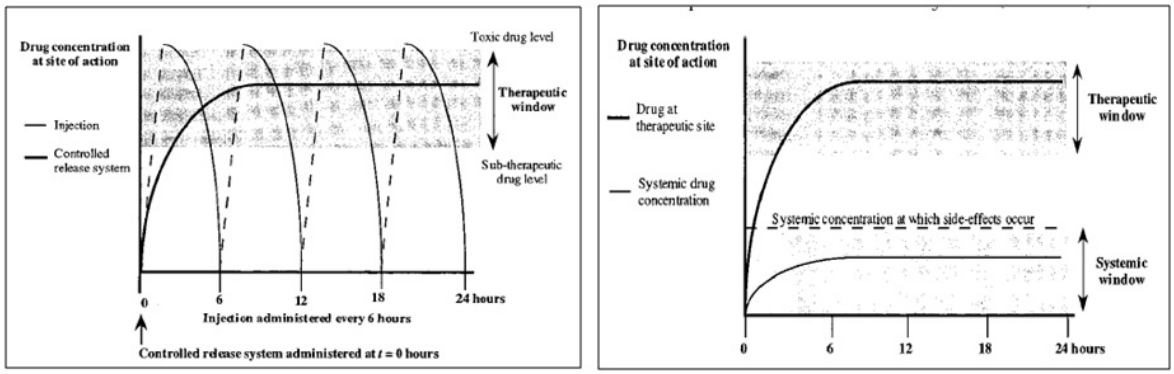

*FIGURE 1.1(a) Drug concentrations at site of therapeutic action after delivery as a conventional injection (thin line) and as a controlled release system (bold line) (b) Drug delivery from an ideal controlled release system. Bold line: Drug concentrations at site of therapeutic action. Thin line: Systemic levels at which side effects occur.(adapted from Uhrich, K.E.; Canizzaro S.M.; Langer,R.; Shakesheff, K.M. Chem. Rev., **1999**, 99, 3181)*

Figure 1.1 shows that in case of the controlled release system, the rate of drug release matches the rate of drug elimination thus, ensuring that the drug concentration stays well within the therapeutic window for a reasonably longer time [5]. Controlled release formulations are widely employed in cancer therapy because of the low water solubility and poor selectivity of anticancer drugs. The possibility of creating drug delivery systems able to determine both controlled release of the drug, through optimization of its pharmacokinetics, and drug targeting, through a moiety able to drive the carried drug to specific organs and tissues, rapidly became a primary goal, especially in cancer chemotherapy. Figure 1.2 shows the common strategies for the delivery of chemotherapeutic agents. The release of a pharmaceutical agent can be controlled by encapsulation within a polymer, lipid or surfactant thereby improving the efficacy of the drug. [6] Since then, polymers with varying chemical and biological properties have been investigated in an effort to achieve long circulation times, slow release, and/or targeting of the conjugated drugs, thus improving their therapeutic use. [7]

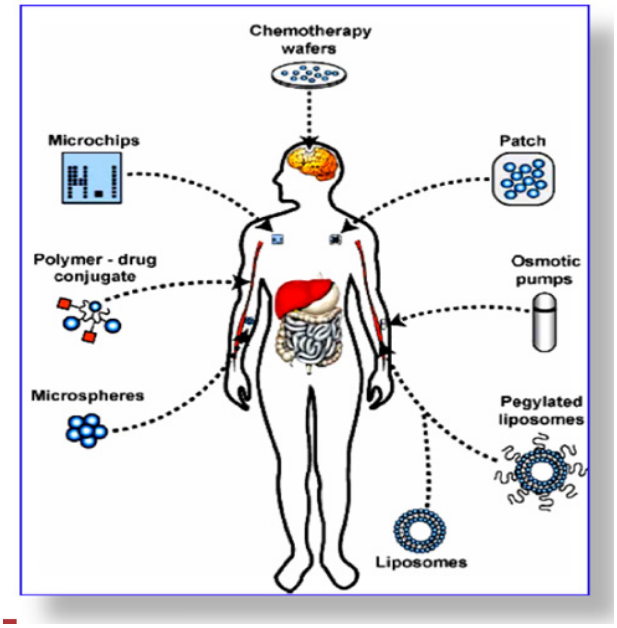

Figure 1.2 shows the common strategies for the delivery of chemotherapeutic agents.

1.2. POLYMERS AS DRUG CARRIERS AND EPR EFFECT

Polymeric self-assembled structures have gained considerable interest in the past decade in the biomedical field especially in the field of drug targeting, contrast enhancement and as materials for nanocoatings. These nanomedicines enhance existing treatments owing to controlled release rate, prolonged circulation and hence,

increased therapeutic effect. These ‘nanovehicles’ also offer certain other privileges like high loading capacity, adequate stability in the bloodstream, long circulating properties and selective drug targeting. Nanoparticles made from biodegradable polymers have been widely investigated for long term delivery of drugs since they offer unique advantages like prolonged bioactivity, lesser side effects, decreased administration frequency, thereby facilitating patient compliance.[7]

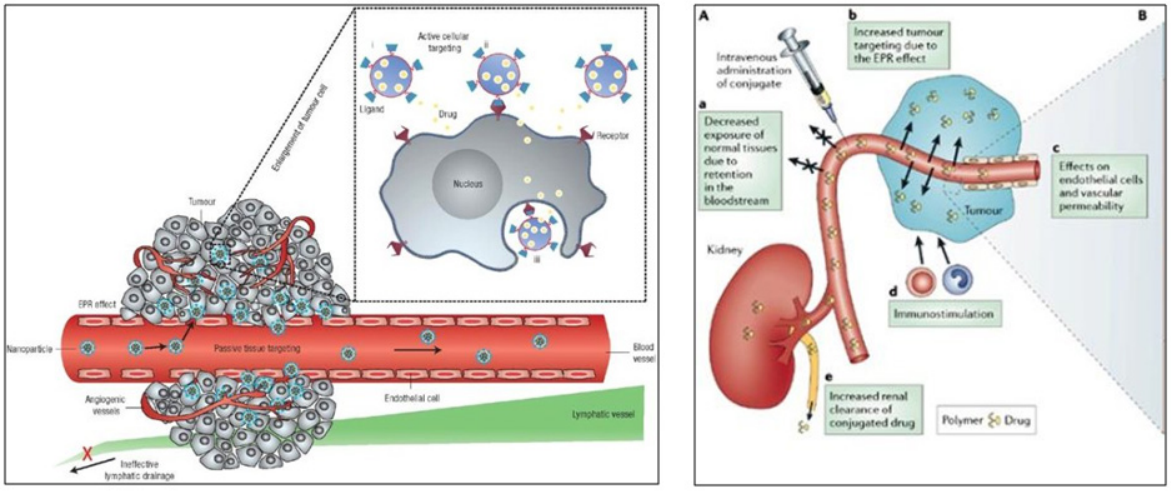

FIGURE 1.3: The Enhanced Permeation and Retention (EPR) Effect(Duncan, R. *Nat Rev Cancer* **2006**, *6*, 688-701.

It has been well-established now that long circulating molecules like albumin, polymer conjugates, polymer micelles and liposomes accumulate in tumour cells via a passive targeting phenomenon, the EPR effect. This can be attributed to two factors: the disorganized pathology of the tumour vasculature during the course of angiogenesis that gives rise to a discontinuous epithelium leading to the hyper permeability of circulating macromolecules and the lack of effective lymphatic drainage that result in their gradual accumulation. Once present in the tumour interstitium, the nanocarriers are internalized through the endocytotic pathway or by pinocytosis.[8] Figure 1.3 explains the Enhanced Permeation and Retention (EPR) effect. In the recent past, synthetic and natural polymers are being extensively used for drug delivery applications. Some common synthetic amphiphilic copolymers for drug delivery applications include poly (lactic acid)-block-poly ethylene glycol (PLA-b-PEG), poly (l-lactide)-block-poly ethylene oxide (PLL-b-PEO), poly ethylene glycol-poly 2-vinyl pyrrolidine(PEG-P2VP), polystyrene-block-poly ethylene oxide(PS-b-

PEO) etc. Commonly used polymers for drug delivery related applications are shown in Figure 1.4.

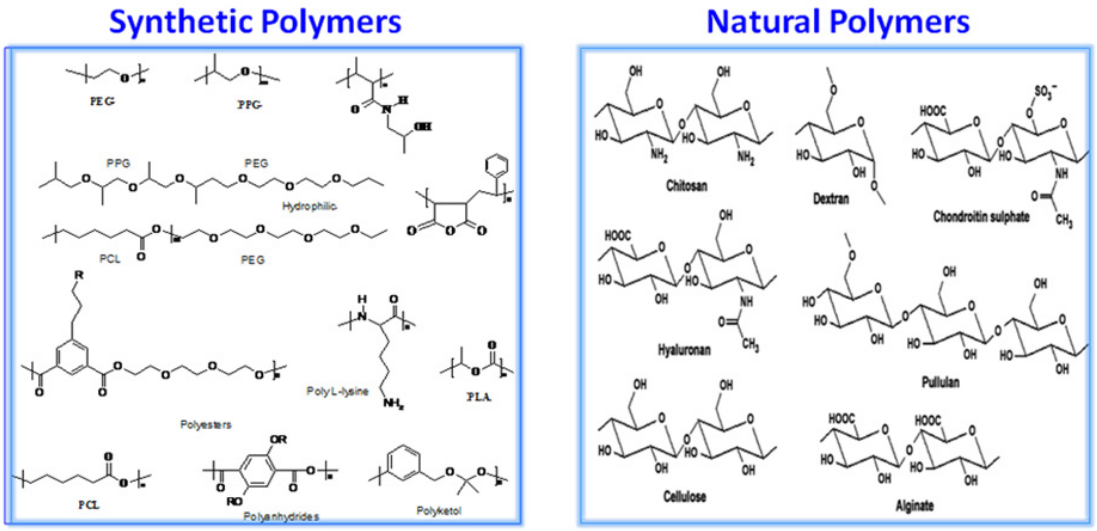

FIGURE 1.4 shows some commonly used polymers for drug delivery applications (adapted from Progress in Polymer Science 34 (2009) 1261–1282)

The biodegradability and biocompatibility of synthetic polymers is debatable due to the presence of a carbon-carbon backbone. Natural polymers like carbohydrates, offer the inherent advantage of being biodegradable under physiological conditions though enzymatic or oxidative cleavage and are biocompatible. Of the naturally available polymers, chitosan, pullulan, alginate, hyalanuric acid etc. have been exploited for drug delivery. Dextran, obtained from bacteria has also been hydrophobically modified to obtain nanoscaffolds. Pramod et al. from our research group have modified dextran to obtain vesicles and have also encapsulated hydrophilic and hydrophobic molecules in the vesicular scaffold. However, the availability of the above biopolymers limits their applications since they are not abundant unlike starch and cellulose.

1.3. STARCH BASED DRUG DELIVERY VEHICLES

Natural polymers are poly-hydroxy aldehydes or ketones with the general formula $(CH_2O)_n$. They are ubiquitous in nature and they perform a plethora of functions. In addition to the inherent configurational variation (glucose/mannose), additional variety caused by ring size, branching, anomeric configuration and modifications gives strong potential for diversity. This inherent structural diversity parallels a wide range of functions within nature, ranging from a source of energy

and metabolic intermediates to the structural components of plants (cellulose), animals (chitin), and nucleic acids (DNA, RNA). Starch is an abundant, inexpensive naturally occurring polysaccharide and is the major form of stored carbohydrate in plants such as corn, wheat, rice, and potatoes. Cellulose constitutes the structural components of cell walls of plants and is responsible for its integrity.[9] Peptidoglycan, a glycoprotein is an important constituent of the cell wall of bacterium. In fact, antibiotics target the disruption of the process of peptidoglycan synthesis to kill bacteria. Some glycoproteins have been reported to exhibit a pivotal role in processes as diverse as fertilization, neuronal development, hormone activities, immune surveillance, and inflammatory responses. The carbohydrates of host cells are often employed by pathogens for cell entry and immunological evasion.[10] Cellulose is a polysaccharide consisting of linear β-D- glucose units linked in 1, 4 position. However, it cannot be employed for administration of drugs since humans cannot digest cellulose owing to the absence of the enzyme cellulase. [11] Hence, there has been a growing interest in modified derivatives of starch for biomedical applications.

Native starch is a mixture of two polyglucans namely: amylose and amylopectin consisting of α-D-Glucose units linked in 1,4 –position. In most common types of starch, the weight percentages of amylose range from 72% to 82% and the amylopectin content varies from 18% to 28 %. Amylose is nearly unbranched and has a molecular weight of 10^5-10^6. Amylopectin is highly branched with the branches connected at the 1, 6 linkage of the anhydro glucose unit and has a very high molecular weight of 10^6-10^7. [12]

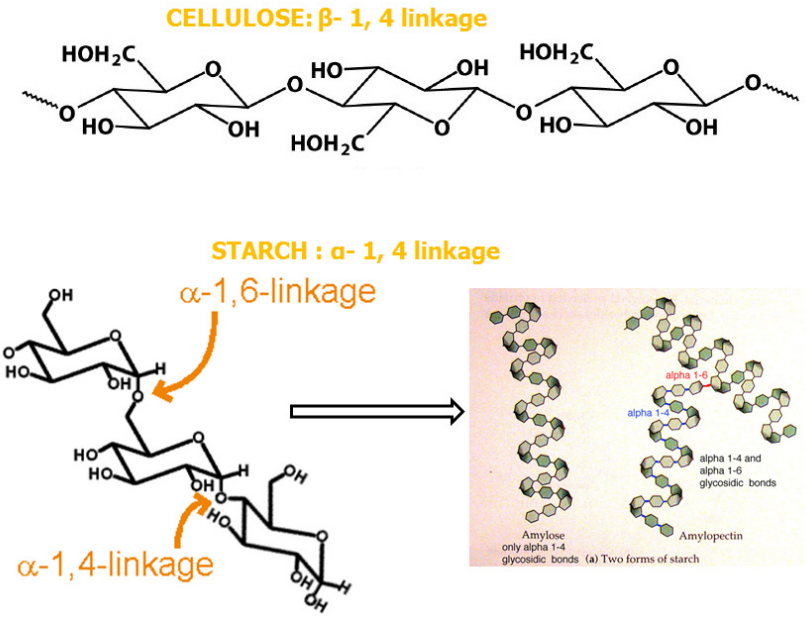

FIGURE 1.5 shows the constituents of starch namely: amylose and amylopectin and the conformational differences between starch and cellulose

For it to be used as a drug carrier, starch has to be hydrophobically modified. It has been reported that epichlorohydrin cross-linked amylase starch was used as a matrix for the controlled release of contramid. [13] Starch graft copolymers such as starch-*g*-polymethylacrylate and starch-*g*-polystyrene have been synthesized by generating free radicals on starch and reacting these free radicals with the respective vinyl monomers.[14a] However, these copolymers with vinyl polymer branches also have limited biodegradability because of the presence of their nondegradable branch units, although their properties are acceptable for applications. An interesting approach comprises a surface modification of the superficial OH groups of starch by coupling the reaction with e.g. phenyl isocyanate, which could change certain properties of material without changing its bulk characteristics. But isocyanates are considered to be hazardous to the environment.[14b] The high hydrophilicity and molecular weight, poor processability and solubility in common organic solvents limit wide applications of starch. [15]

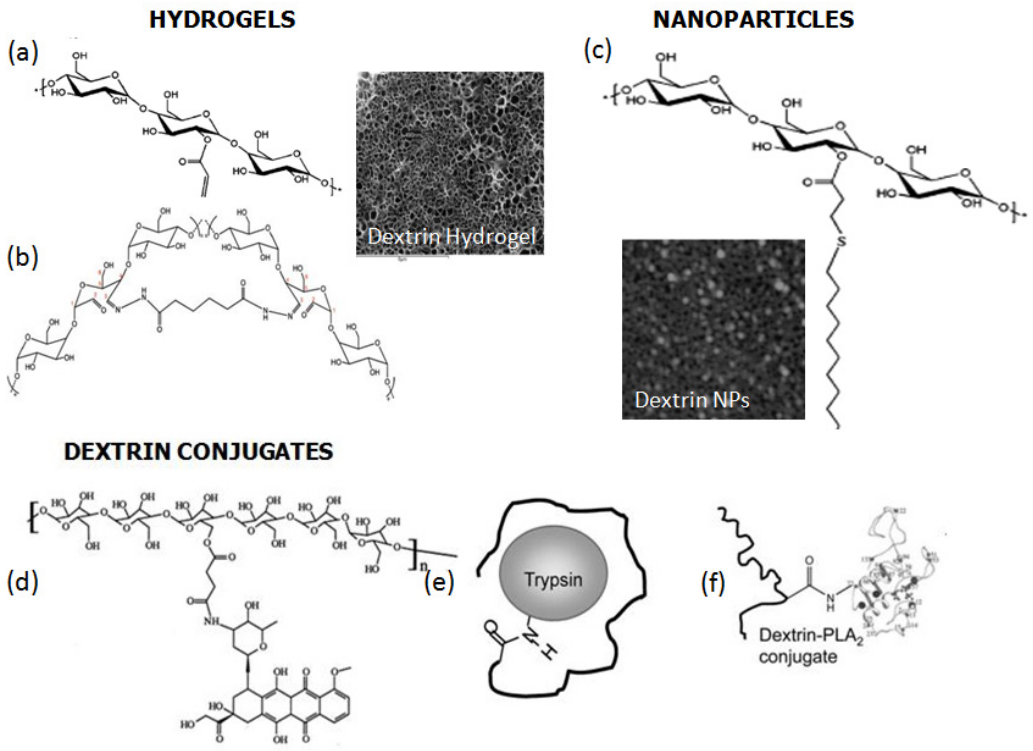

SCHEME 1.1 shows (a) hydrogels of dextrin-vinylacrylate and oxidized dextrin and their corresponding cryo-SEM image (b) dextrin-hexadecanethiol nanoparticles and the corresponding AFM image (c) dextrin conjugates

As mentioned earlier, the high molecular weight of starch makes its modification difficult. Instead, starch is hydrolysed to obtain a polymer of moderate molecular weight which can be functionalized easily. Dextrin is a glucose containing saccharide polymer linked by α 1,4-linked (> 95%) D-glucose units having the same general formula as starch but it is smaller and less complex with minimal branching in the α 1,6-position(<5%). It is produced by partial hydrolysis of starch using acid, enzymes or a combination of both. It is readily degraded within minutes by α-amylase present in human saliva and pancreas to produce maltose and isomaltose. [16] Dextrin is approved for clinical use as the peritoneal dialysis solution (Icodextrin), as a solution to prevent postoperative adhesions (Adept) and as a formulation solution for peritoneal administration of 5-fluorouracil. Duncan et al. synthesized dextrin-doxorubicin; dextrin-tyrosinamide and dextrin-biotin conjugates through succinoylation of dextrin and the rate of degradation of dextrin-doxorubicin conjugates by amylase could be tuned by changing the degree of succinoylation.[17] Carvalho et al. synthesized dextrin-vinyl acrylate hydrogels and dextrin hydroxyethylmethacrylate and investigated their cytotoxicity and degradability profiles.[18] In another report, Duncan et al. have reported the synthesis of a dextrin-rhEGF conjugates to promote tissue repair since α-amylase is known to be present in wound fluids and it was found that the conjugate was able to stimulate *in-vitro* proliferation and migration of keratinocytes and fibroblasts that aid wound healing.[19] Dextrin-trypsin and dextrin-PLA_2 conjugates were explored to demonstrate the feasibility of using dextrin for protein/anticancer drug masking with unmasking possible through addition of α-amylase. [20],[21] Gonçalves et al. have developed a method to synthesize and characterize dextrin-based nanogel by the Michael addition reaction of dextrin-vinyl acrylate and 1-hexadecanethiol and have employed it to encapsulate a hydrophobic drug, curcumin. [22] The nanogel so obtained had high colloidal stability. In another work, dextrin based hydrogels have been reported to effectively incorporate and stabilize a recombinant mutated interleukin-10 (rIL-10), allowing for the release of biologically active rIL-10 over time. [23]

In most of the literature reports, modified dextrins were found to be self-organized as nanoparticles or micelles; as a result polysaccharide vesicles are less explored for drug delivery. Hence, dextrin based polysaccharide vesicles are important and the design of dextrin based vesicles is a synthetic challenge in itself and relevant in the context of drug delivery applications since vesicles are higher order structures

and offer dual encapsulation capabilities i.e. both hydrophilic and hydrophobic molecules can be loaded in the vesicular scaffold. Moreover, they show enhanced cellular uptake since they mimic the cell membrane and hence, are internalized through like interactions.

1.4. AIM OF THE THESIS

In this study, we have designed and synthesized dextrin-amphiphiles from two biodegradable, renewable resources namely Dextrin, obtained from the hydrolysis of starch and 3-Pentadecylphenol that is obtained from cashew nut shell liquid. The aim was to employ them as drug delivery vehicles. Moreover, the role of the hydrophobic unit in the self assembly was assessed that gives an insight into the forces that play at the molecular level and give rise to these self assembled structures. (See figure 1.6)

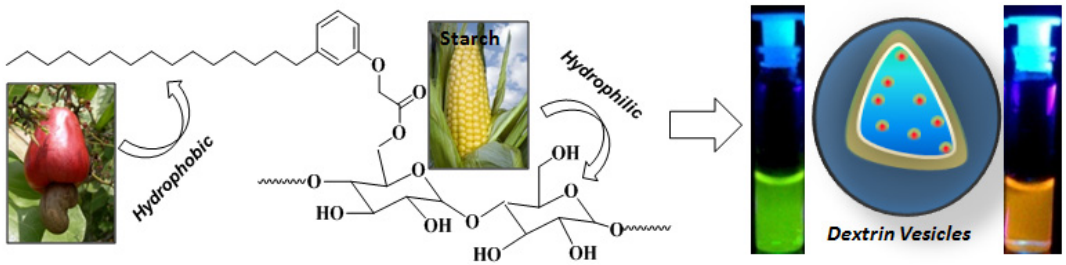

FIGURE 1.6 shows the constituents of DEX-PDP scaffolds and their self assembled structure

The novelties of the present thesis can be summarized as follows: Custom designed amphiphile was synthesized from renewable resources though a facile, tailor made approach. The Degree of substitution of hydrophobic unit on the dextrin backbone was varied from 5 to 50%. Vesicular scaffolds with diameters ranging from 160-500 nm were synthesized with varying degree of substitutions using a simple DCC/DMAP coupling reaction. The role of the hydrophobic unit in the self assembly process was studied. The scaffolds so obtained were characterized by NMR and FT-IR. Their self assembly was confirmed by DLS, SEM, TEM, fluorescence and AFM techniques. The encapsulation abilities of the scaffolds were studied using a model dye, Rhodamine-B. The in-vitro release characteristics of Rh-B encapsulated within DEX-PDP-7 vesicles was studied under physiological conditions.

MATERIALS AND METHODS

2.1. MATERIALS

Dextrin (Type 1 from corn, M_w=7700 g/mol), 3-pentadecylphenol, dicyclohexyl carbodiimide, 4-dimethylaminopyridine, pyrene, rhodamine-B and horse liver esterase were purchased from Aldrich Chemicals. Dry DMF was purchased from Finar reagents and distilled using calcium chloride and calcium hydride. Ethyl chloroacetate, K_2CO_3, KOH, and other solvents and reagents were purchased locally and purified following the standard procedure.

2.2. METHODS

NMR was recorded in a 400 MHz Jeol NMR spectrometer in $CDCl_3$ (for PDP-ester) and dmso-d_6 (for PDP-acid and DEX derivatives) containing a small amount of TMS as internal standard. FT-IR spectra of all compounds were recorded on a Thermo Scientific Nicolet 6700 FTIR spectrometer using potassium bromide (KBr) disks prepared from powdered samples (3 mg) mixed with dry KBr. The spectra were recorded in absorbance mode from 4000 to 400 cm^{-1}. Thermal gravimetric analysis (TGA) was performed on a Perkin Elmer STA 6000 instrument. Mass of PDP-derivatives was confirmed using the Applied Biosystems 4800 PLUS MALDI TOF/TOF analyzer. Absorption and Emission studies were performed on a Perkin-Elmer Lambda 45 UV-Visible spectrophotometer and SPEX Flurolog HORIBA JOBIN VYON fluorescence spectrophotometer with a double grating 0.22 m spex 1680 monochromator and a 450 W Xe lamp as the excitation source at RT. The excitation spectrum was collected at 375 and 420 nm and emission was collected by exciting the sample at the excitation maxima. The size of the DEX-PDP amphiphiles was determined by DLS using a Nano ZS-90 apparatus using a 633 nm red laser at 90 ^{o} angle from Malvern instruments. The sample was dispersed in water (or PBS) to obtain a concentration of 0.5 mg/ml and then sonicated, heated and filtered using a 0.45 µm filter to afford a clear solution. For the DEX-PDP derivatives encapsulated with Rhodamine-B, the solution from the dialysis bag was filtered and diluted before analysis.AFM images were recorded by drop casting the samples on a freshly cleaved mica surface using Carl Zeiss AFM setup and the experiment was performed in tapping mode.FE-SEM images were recorded on a Zeiss Ultra Plus scanning electron microscope with samples prepared by drop casting on a silicon

wafer and air dried.TEM images were recorded using a Technai-300 instrument by drop casting and air drying the sample on formvar coated copper grid.

2.3. GENERAL PROCEDURES

2.3.1. Synthesis of Ethyl 2-(3-pentadecylphenoxy) acetate (PDP-ester, 1a): To a stirring solution of 3-pentadecylphenol (10 g, 0.03289 mol) in DMF (70 ml) was added K_2CO_3 (9 g, 0.06578 mol). The mixture was stirred at 90^oC for 1 hour under nitrogen atmosphere. The reaction mixture was then cooled to RT and ethyl chloroacetate (5.2 ml, 0.0493 mol) was added dropwise. The reaction was then allowed to stir for 24 hours at 90^oC under nitrogen atmosphere. The reaction mixture was poured into water (150 ml) and extracted using ethyl acetate (100 ml x 2). The organic layer was washed with NaOH, dried over anhydrous sodium sulphate and the solvent was removed under reduced pressure to afford a low melting solid. It was further purified by a silica gel column using 2 % ethylacetate-hexane system as the eluent. Yield= 10g (77 %).^{1}H NMR (400 MHz, $CDCl_3$) δ: 7.27 ppm (t, 1H, Ar-**H**), 6.80 ppm (d, 1H, Ar-**H**), 6.74 ppm (s,1H, Ar-**H**), 6.69 ppm (d, 1H, Ar-**H**), 4.67 ppm (s,2H,O-**CH_2**), 4.33 ppm (q, 2H, OCH2-**CH_3**), 2.57 ppm (t, 2H, Ar-**CH_2**), 1.52 ppm (m, 2H, Ar-CH_2-**CH_2**), 1.26 ppm (m, 27H,aliphatic-H), 0.87 ppm (t, 3H, -CH_3). ^{13}C NMR ($CDCl_3$, 100 MHz) δ: 169.34 (**C**=O), 158.10,142.04, 129.72, 121.776, 115.01, 112.08 (Ar-**C**), 65.06 (Ar-O-**C**H2), 61.07 (O-**C**H2-CH3),35.68, 31.83, 31.42, 29.57, 29.41, 29.26, 22.63 and 14.48. FT-IR ((KBr), cm-1), 3037, 3006 (Aromatic C-H stretch), 2925, 2854 (Aliphatic C-H stretch), 1762 (Ester C=O stretch), 1585 (ring C=C stretch), 1201 (C (=O)-O stretch) MALDI TOF/TOF, (MW: 390), m/z=429 (M+K+).

2.3.2. Synthesis of Ethyl 2-(3-pentadecylphenoxy) acetic acid (PDP-acid, 1 b): To a solution of PDP-ester (5 g, 0.0127 mol) dissolved in dioxane (30 ml) was added KOH (2.18 g, 0.0383 mol). The reaction mixture was refluxed for 24 hours at 105^oC under nitrogen atmosphere. The reaction mixture was poured into water (150 ml), acidified with dilute hydrochloric acid until the pH became 4 and extracted into ethyl acetate (100 ml).The organic layer was washed with brine, dried over anhydrous sodium sulphate and the solvent was removed under reduced pressure to afford a fluffy, white solid that was further recrystallized from methanol. Yield : 4.6g (96%). ^{1}H

NMR(400 MHz, dmso-d_6) δ: 7.14 ppm (t, 1H, Ar-**H**), 6.67 ppm (m, 3H, Ar-**H**), 4.52 ppm (s, 2H, O-**CH_2**), 2.52 ppm (t, 2H, Ar-**CH_2**) ,1.52 ppm (m, 2H, Ar-CH2-**CH_2**), 1.27 ppm (m, 27H, Aliphatic protons). ^{13}C NMR (dmso-d_6, 100 MHz) δ: 170.79 (CO-OH), 158.23, 144.46, 129.66, 121.52, 115.00, 111.90 (Ar-**C**), 64.83(O-**C**H2), 35.68, 31.83, 31.46, 29.57, 29.26, 22.63,14.48 (Aliphatic-**C**)FT-IR ((KBr), cm-1), 3093, 3043 (Aromatic C-H stretch), 2956, 2919, 2848 (Aliphatic C-H stretch), 1731 (Acid C=O stretch), 1577 (ring C=C stretch), 1421 (O-H bending), 1272 (C (=O)-O stretch). MALDI TOF-TOF, (MW: 362.5), m/z= 401.5 (M+K+).

2.3.3. Synthesis of DEX-PDP-x: Dextrin (type 1 from corn, Mw=7700, 0.5 g, 0.00310 mol of anhydroglucose unit) was dissolved in 20 ml dry DMF and refluxed for 1 hour at 90^{o}C under nitrogen atmosphere. It was then cooled to RT and purged with nitrogen for 10 min. Following this, PDP-acid (0.57 g, 0.00155 mol for DEX-PDP-13) dissolved in dry DMF (3 ml) was added to the reaction mixture and it was cooled to 0^{o}C. DCC (0.39 g, 0.00186 mol) and 4-DMAP (0.047 g, 0.000310 mol) were added to the reaction mixture and the reaction mixture was stirred at 90^{o}C for 24 hours under nitrogen atmosphere.

The reaction mixture was cooled, filtered to remove dicyclohexylurea and the filtrate was poured into ice-cold methanol. The precipitate was then filtered and washed with methanol. It was dissolved again in DMF and precipitated using methanol and dried in the vacuum oven to afford a crystalline brown solid. Yield=50 %.

^{1}H NMR(400 MHz, dmso-d_6): 7.13 ppm (t, 1H, Ar-**H**), 6.67 ppm (m, 3H, Ar-**H**), 5.42,5.50 ppm(s,2,3-hydroxyl of dextrin), 4.72 ppm (s, 2H, O-**CH_2** of ester linkage), 2.49 ppm (t, 2H, Ar-**CH_2**) ,1.52 ppm (m, 2H, Ar-CH_2-**CH_2**), 1.28 ppm (m, 27H, Aliphatic protons), 0.87 ppm (s, 3H, -CH_3).

FT-IR ((KBr), cm-1): 3438 (O-H stretch), 2922, 2852 (Aliphatic C-H stretch), 1765 (Ester C=O stretch), 1693 (ring C=C stretch), 1450 (O-H bending), 1207 (C (=O)-O stretch).

DEX-PDP with different degree of substitutions i.e DEX-PDP-7, 13, 25, 33 and 50 were thus, synthesized by changing the mole ratio of dextrin to PDP-acid as 0.25, 0.5, 1, 1.5 and 2 in the feed.

2.3.4. Determination of critical vesicular concentration (CVC): The critical vesicular concentration was determined using Pyrene as a probe. In a typical experiment, 1 ml of Pyrene in acetone (0.6 µM) was added to 3 ml glass vials and the acetone was allowed to dry completely. Concentrations of DEX-PDP derivatives varying from 0.5 mg/ml to 0.00033 mg/ml were then added to these vials. The vials were sonicated for 1 hour and the samples were left to equilibrate overnight. The excitation wavelength was set to be 334 nm and the excitation and emission slit width were fixed as 3 nm.

The ratio of fluorescence intensity at I_1 (375 nm) and I_3 (386 nm) was calculated and plotted against the logarithm of concentration to obtain a graph where the onset of the slope gave the critical vesicular concentration (CVC).

2.3.5. Encapsulation of a hydrophilic dye Rhodamine (Rh-B) in DEX-PDP vesicles: The ability of the DEX-PDP-derivatives to stabilize Rh-B was investigated using the solvent exchange/dialysis method. In a typical experiment, 20 mg of the polymer and 2 mg of Rhodamine-B was dissolved in 2 ml DMSO. Following this, 2 ml of distilled water was added drop wise into the polymer solution stirring at 25^{o} C and further stirred for 12 hours. The solution was transferred to a dialysis bag(MWCO=2000), stirred for 24 hours and dialyzed against distilled water upto 7 days to check the stabilization of the hydrophilic dye.

2.3.6. *In vitro* studies: To study the release profile of Rh-B, 3 ml of the solution in the dialysis bag above was immersed in 100 ml PBS buffer (pH 7.4) in a beaker. At specific time intervals, 3 ml of the dialysate was withdrawn and replaced with an equal volume of fresh buffer. The amount of Rh-B present in each aliquot was measured using UV-Visible spectroscopy and quantified using Beer-Lambert's law in terms of weight percentage. To ascertain the effect of esterase enzyme on the Rh-B, 10 U of horse liver esterase was added to the dialysis bag and the above procedure was repeated.

RESULTS AND DISCUSSION

3.1. SYNTHESIS OF DEX-PDP DERIVATIVES AND CHARACTERIZATION

Dextrin (type 1 from corn, M_w= 7700 g/mol), a biocompatible and biodegradable starch-based polymer obtained from the hydrolysis of corn starch was grafted with a renewable resource, 3-pentadecylphenol (PDP), a prime constituent of cashew nut shell liquid as the hydrophobic side chain using a DCC/DMAP coupling (See Scheme 3.1). Briefly, 3-pentadecylphenol was reacted with ethyl chloroacetate in the presence of K_2CO_3 as base to give ethyl 2-(3-pentadecylphenoxy) acetate (**1a**). The ester bond in **1a** was hydrolysed using KOH to give ethyl 2-(3-pentadecylphenoxy) acetic acid(1b). **1b** was then coupled with dextrin to afford DEX-PDP. ^{1}H-NMR spectrum of PDP-ester (see figure 3.1) (in $CDCl_3$) showed peaks from 6.77-7.27 ppm corresponding to the aryl protons. While the peak at 4.67ppm was designated to the Ar-**OCH_2**, the peak at 4.33 was assigned to the Ar-OCH_2-COO-**CH_2**-CH_3. Upon conversion to PDP- acid, the peak at 4.33 vanished which confirmed the cleavage of the ester and formation of acid. (See figure 3.1). PDP-acid thus, obtained was conjugated to dextrin by DCC/DMAP coupling reaction.

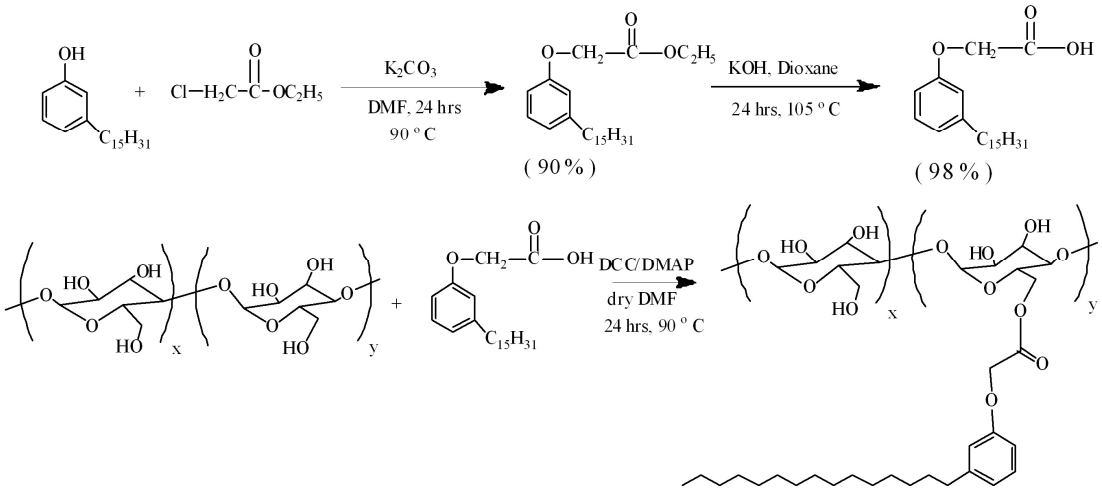

SCHEME 3.1: Synthesis of dextrin derivatives

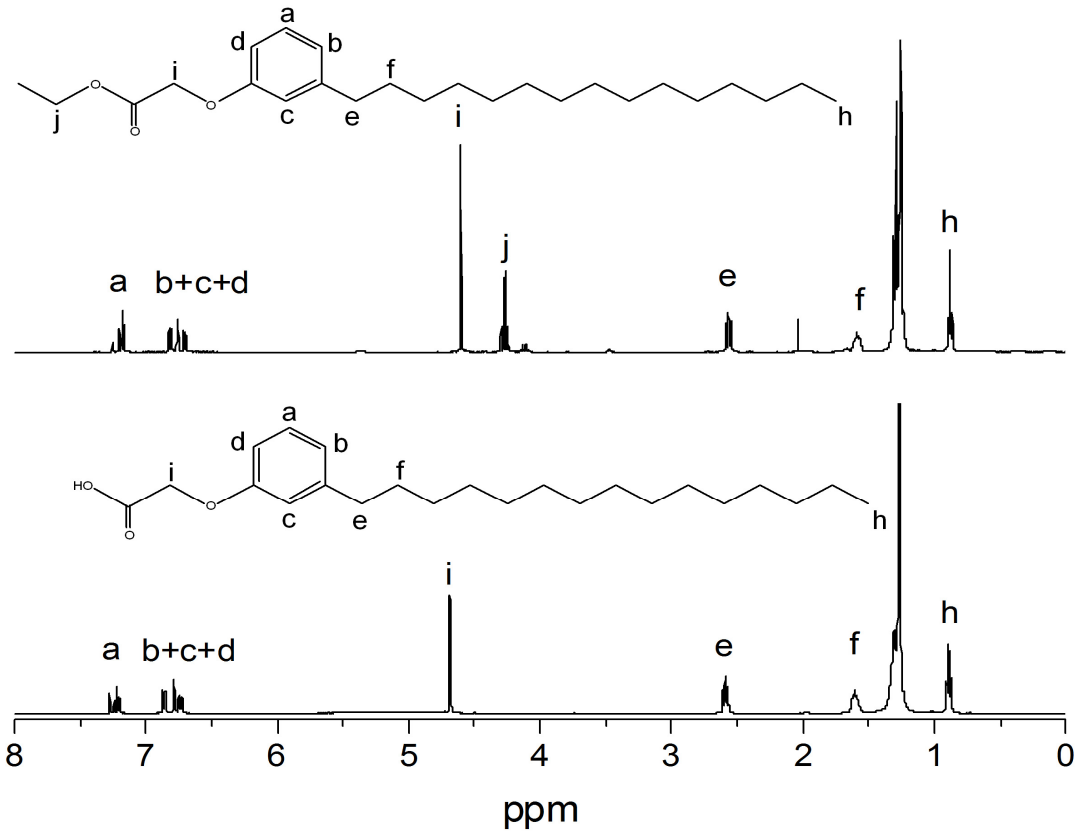

FIGURE 3.1: show the [1]H NMR of PDP-ester (above) and PDP-acid (below)

The derivatives thus obtained were purified by repeated precipitation in methanol dialysed using a semi permeable membrane and characterized by NMR, FT-IR and TGA analysis.

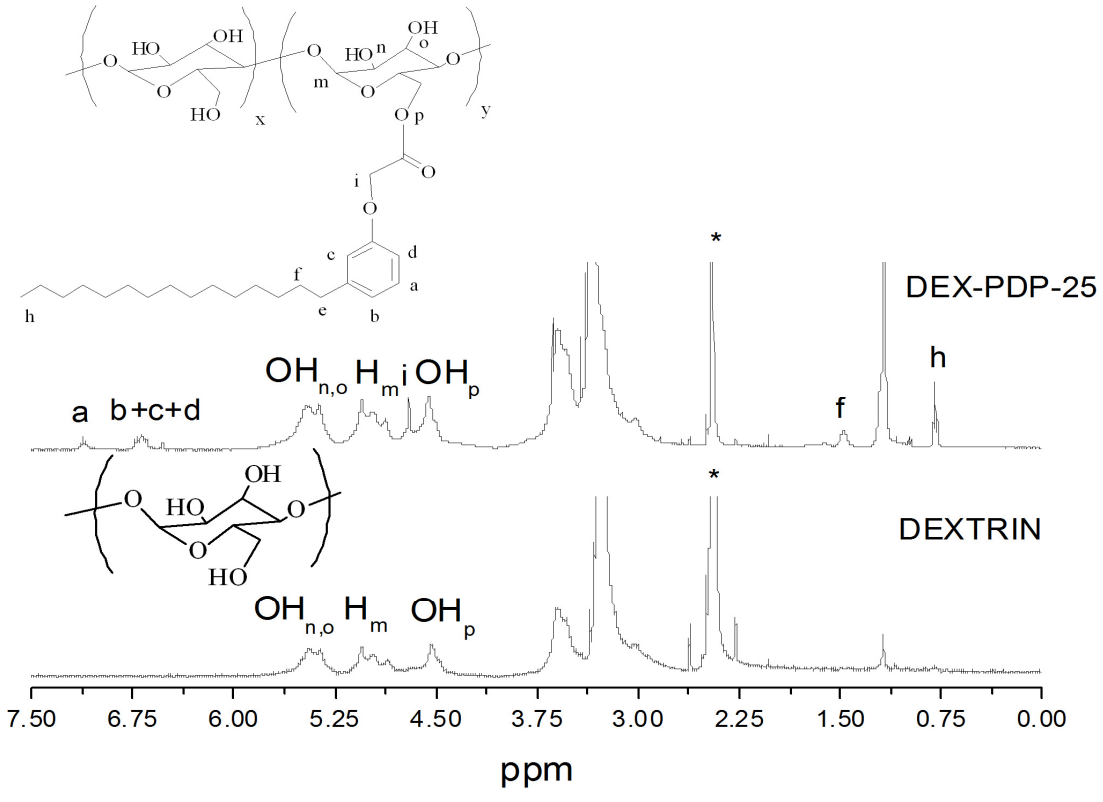

FIGURE 3.2: [1]H NMR of Dextrin and DEX-PDP-25

^{1}H-NMR spectrum of the substituted dextrin showed peaks at 6.67 and 7.13 ppm and 0.5 to 3.00 ppm for the PDP-aryl and aliphatic protons respectively. The protons from dextrin units appeared from 3.30-5.50 ppm. [24] Upon the formation of ester linkage, the protons Ar-**OCH_2**-COO-DEX appeared at 4.67 ppm. (See Figure 3.2)

The degree of substitution (DS) was calculated by comparing the peak intensities of anomeric proton in dextrin at 5.11 ppm with the PDP aryl protons at 7.14 ppm. Figure 9 shows that the intensity of the aromatic peaks increases upon increasing the substitution.

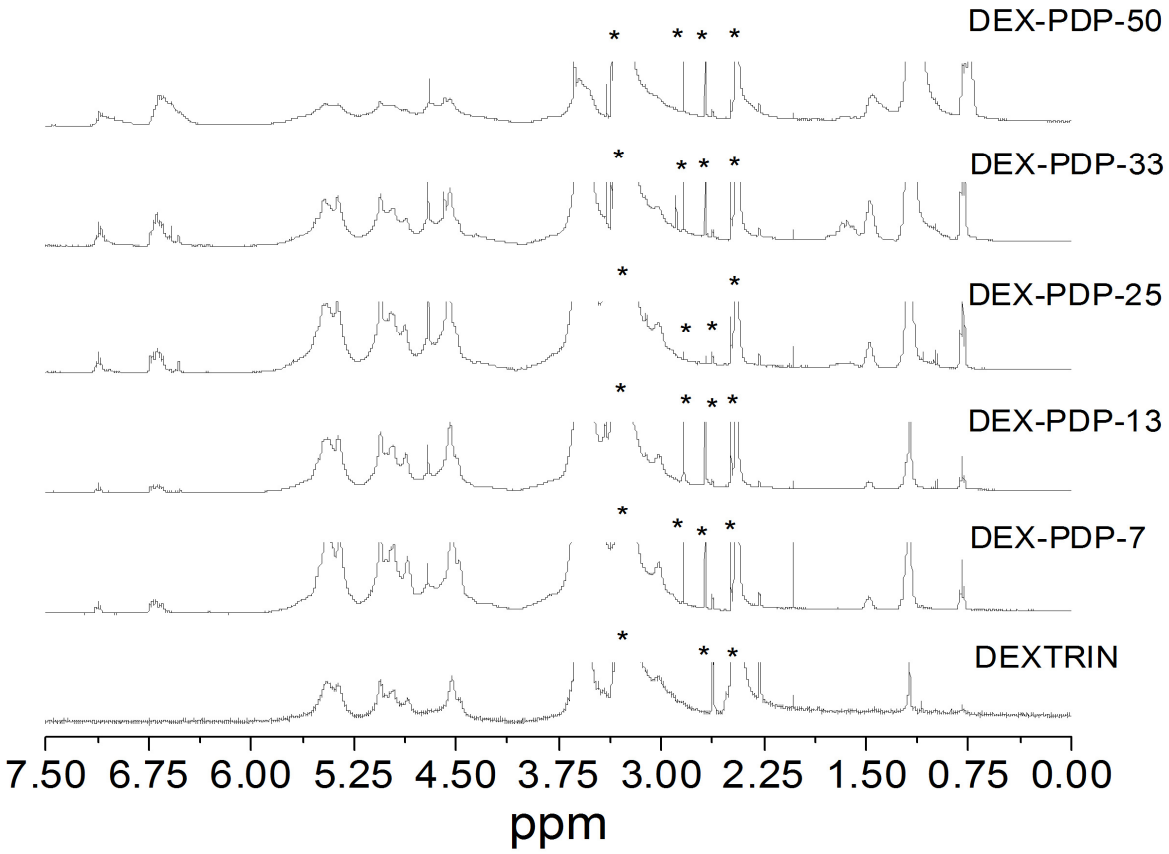

FIGURE 3.3: ^{1}H NMR of Dextrin and DEX-PDP derivatives

A plot of the mole ratio of PDP-acid used versus the degree of substitution showed predominantly a linear trend. (See table 3.1 and Figure 3.4).

Mole percent of PDP-acid	Degree of substitution (%)
20	7
33	13
50	25
60	33
67	50

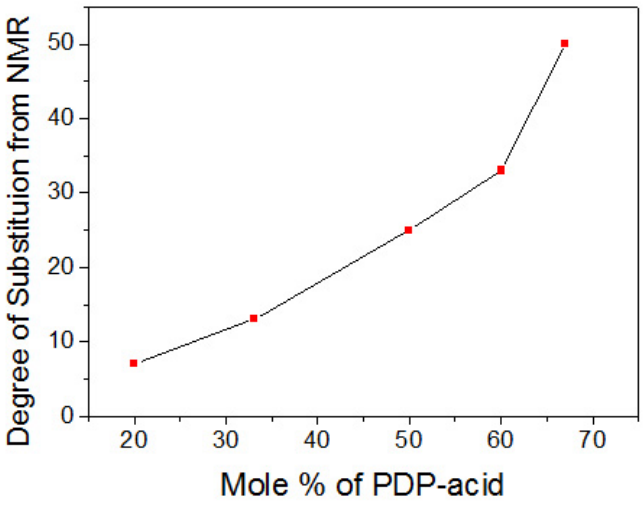

TABLE 3.1 and FIGURE 3.4: shows how the degree of substitution varies with the mole percent

The chemical structure of the amphiphiles was further confirmed using FT-IR technique. FT-IR spectrum of PDP-ester showed a band at 1760 cm^{-1} corresponding to the carbonyl (-C=O stretching frequency) ester linkage (See figure 3.5(a) and (b)). FT-IR spectrum of PDP-acid showed distinct stretching band at 1730 cm^{-1} corresponding to -C=O stretching frequency whereas upon reaction with dextrin, the -C=O stretching frequency shifted to 1765 cm^{-1} corresponding to the ester

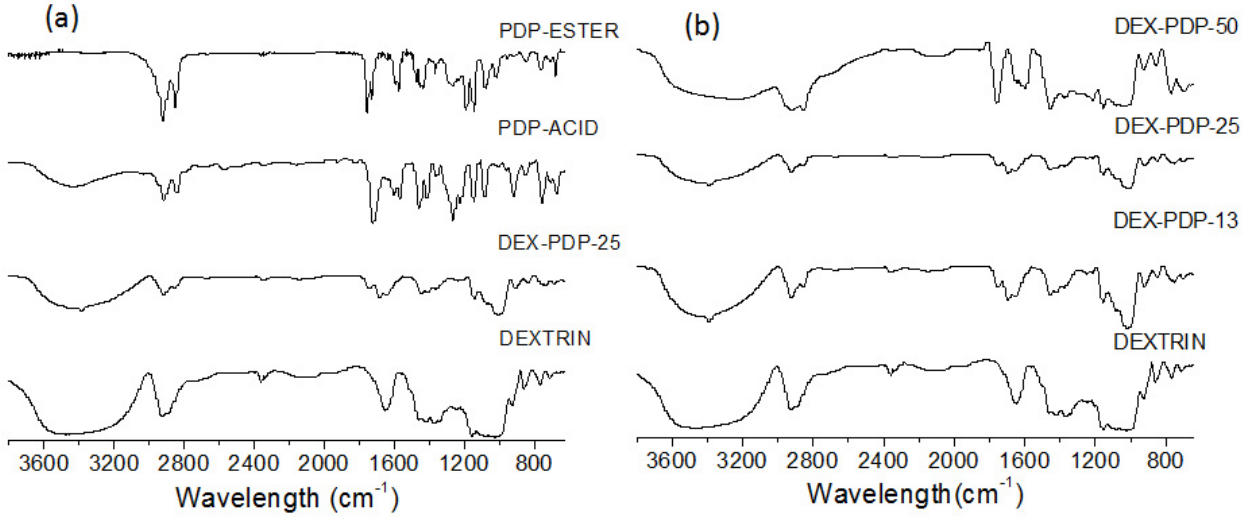

FIGURE 3.5: FT-IR spectrum of DEX-PDP-derivatives

functionality as in the case of PDP-ester. It was also observed that the intensity of the band at 1765 cm^{-1} increased with an increase in the substitution. Thus, the formation of DEX-PDP-derivatives was confirmed by means of NMR and FT-IR

where the suffix ‘x’ stands for the actual incorporation of the hydrophobic PDP unit on the dextrin backbone.

THERMAL CHARACTERIZATION:

The Thermal gravimetric analysis (See Figure 3.6) of the DEX-PDP derivatives showed thermal stability up to 262 ^{o}C with a small increment upon varying the degree of substitution. From the TGA and DSC thermo grams (not shown), it can be concluded that the DEX-PDP derivatives are amorphous in nature.

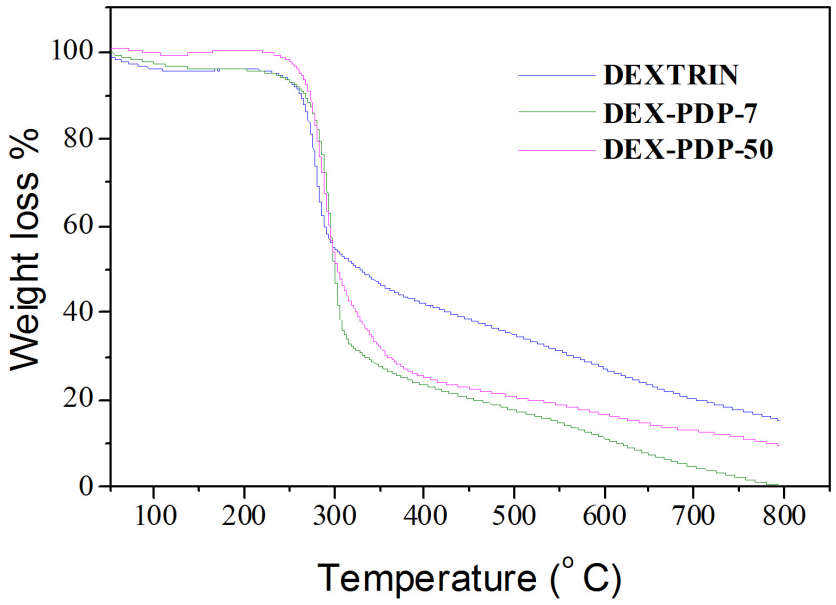

FIGURE 3.6: shows the TGA profile of Dextrin and DEX-PDP -7 ad 25.

3.2. SELF- ASSEMBLY OF DEX-PDP DERIVATIVES

The dissolution of DEX-PDP-x in water is expected to give rise to self-assembled structures due to the amphiphilic nature of the molecule. To determine the hydrodynamic radius of the self assembled structures formed by the DEX-PDP derivatives, they were subjected to Dynamic light scattering (DLS) measurement in water (and PBS buffer). It was found that the lower substitution (DEX-PDP-7) was readily soluble in water whereas the higher substitutions were only partially soluble. Hence, they were filtered before being analysed. The histogram is shown in figure 3.7(a). The DLS profile shows a bimodal, uniform distribution with an average size of 164 nm and a higher order distribution that can be attributed to aggregation. These

derivatives were found to be quite stable under long storage (up to 1 month) as indicated by DLS measurements. The DLS measurement of DEX-PDP-7 was also performed at different concentrations and at different pH values (See figure 3.7a, b and c). At a concentration of 1 mg/ml, the distribution was bimodal and the size was measured to be 164 nm with the presence of some higher aggregates. In randomly modified polymers, the hydrophilic and hydrophobic parts are entangled together and this permits interaction between the core and the aqueous media. The exposed hydrophobic cores within a less mobile shell formed by hydrophilic chains could result in the aggregation of the self-assembled structures that might explain the presence of large macromolecular aggregates in the DLS profile. [25] But at a concentration of 0.2 mg/ml, these aggregates are not observed in the DLS profile. The mean hydrodynamic diameter of DEX-PDP-7 was larger in case of basic solutions than in case of neutral or acidic solutions. The size obtained for pH 4 and pH 7 were in agreement with that obtained in water apart from the presence of smaller particles (20-40 nm) in case of pH 7.

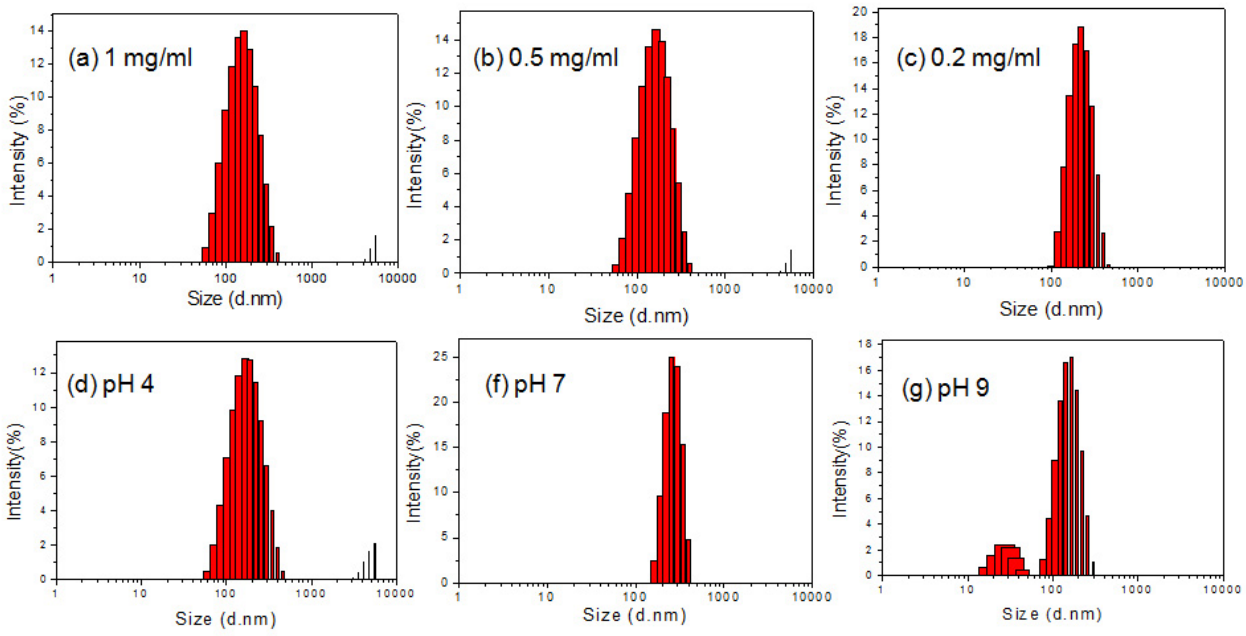

FIGURE 3.7: shows the effect of dilution and pH on the DLS profile of DEX-PDP-7

Also, the average size increased from 164 nm to 500 nm upon varying hydrophobic (PDP) substitution **(**Shown in Figure 3.8).

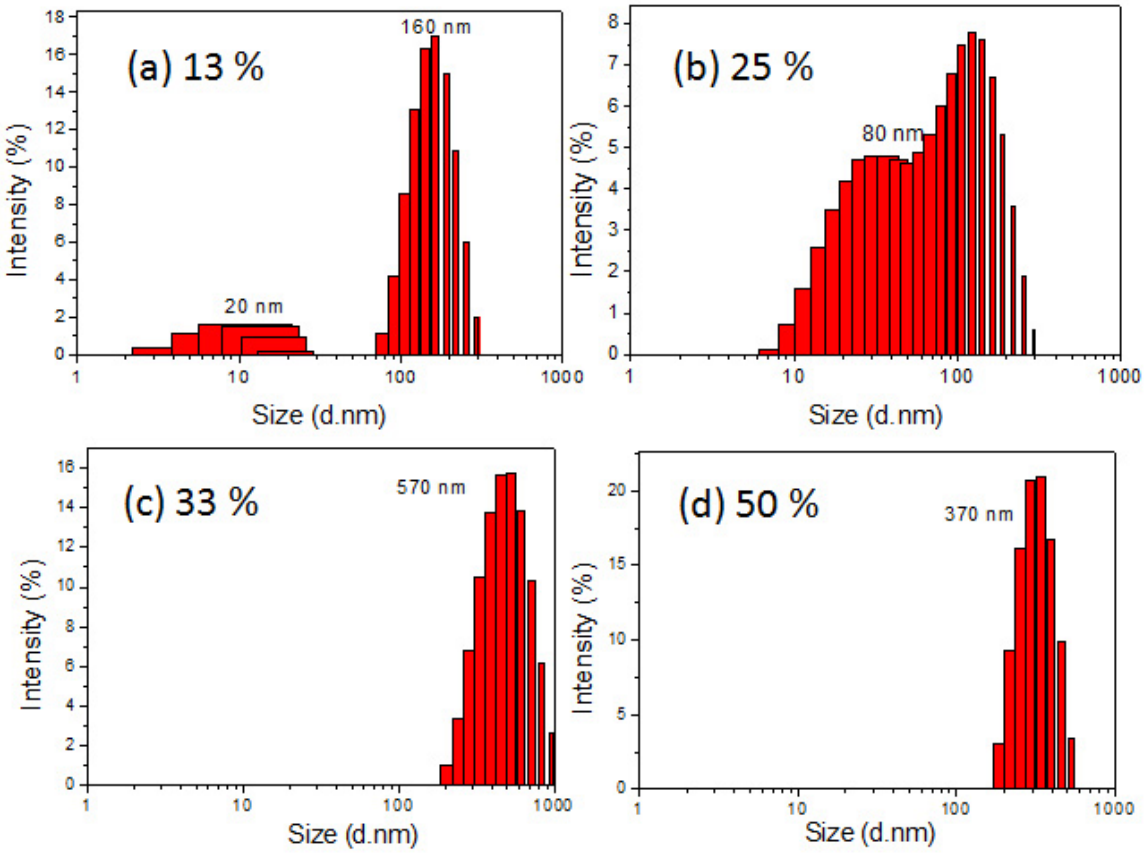

FIGURE 3.8 shows the DLS profile as effect of the degree of substitution

Hence, it can be concluded from DLS that the self assembly of the DEX-PDP derivatives does not appreciably change with dilution or when subjected to different pH. However, it can be observed that it changes drastically upon changing the degree of substitution i.e. it changes from 160 nm to 570 nm upon changing the substitution from 7% to 50 %.

The self- assembly of DEX-PDP amphiphiles was visualized using microscopy techniques. Scanning electron microscopy (SEM) analysis indicates that the morphology of these vesicles in indeed spherical and the corresponding SEM images are given in Figure 3.9. The results obtained from DLS are also in agreement with the size obtained from Scanning electron microscopy (SEM). SEM analysis also revealed that the morphology of the scaffolds changed from vesicular to nanoparticles upon increasing the degree of substitution. HR-TEM (Figure 3.9 e and f) measurements for DEX-PDP-7 indicated the formation of small, unilamellar

vesicles with a dark hydrophilic enclosure surrounding a hydrophilic interior. This

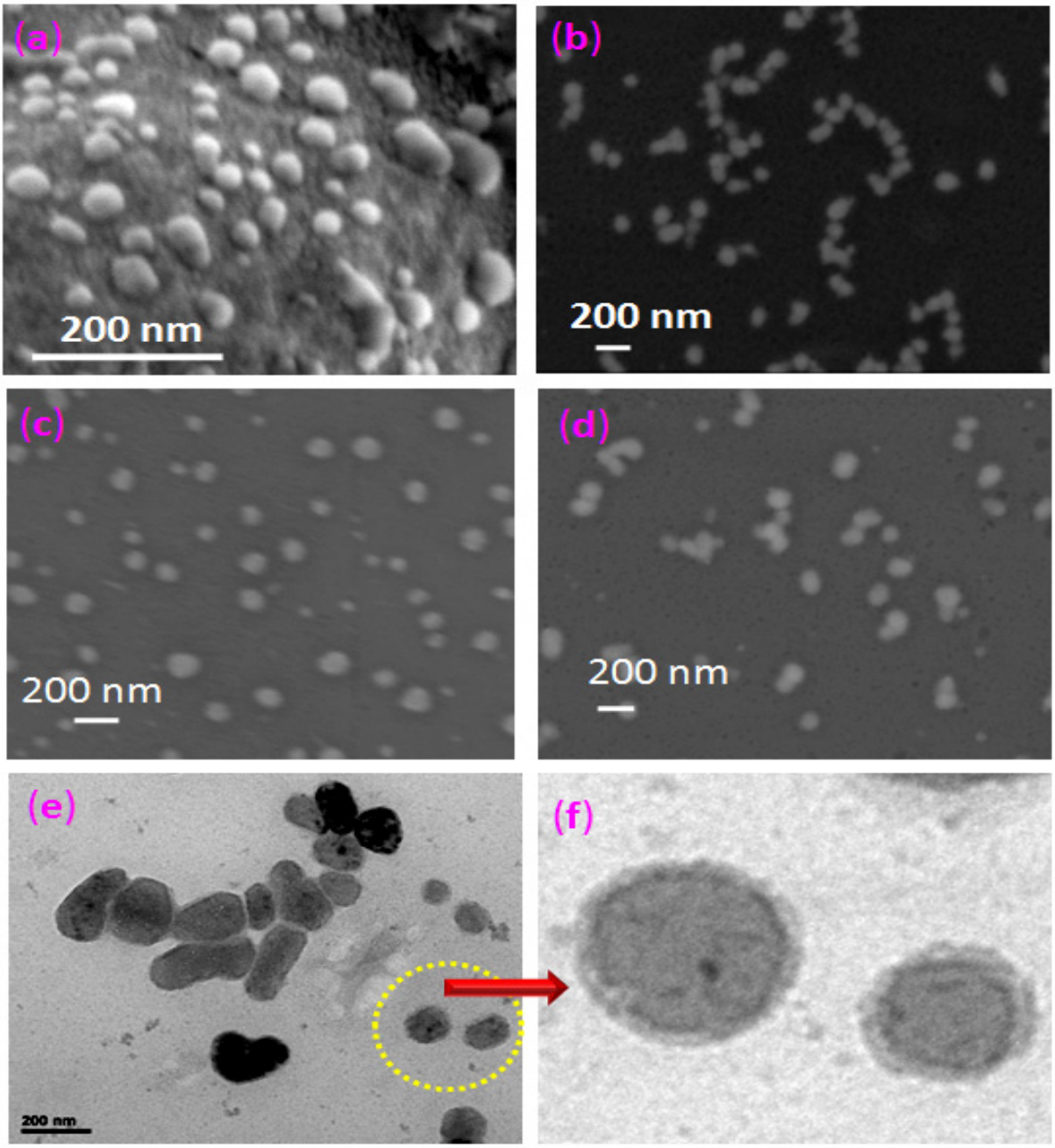

FIGURE 3.9 shows the SEM images of (a) DEX-PDP-7 (b) DEX-PDP-13 (c) DEX-PDP-25 and (d) DEX-PDP-33. (e) Shows the TEM image of DEX-PDP-7 and the enlarged portion (f)

property is unique to vesicular morphologies and also proves to be important evidence to vesicle formation. [26] The wall thickness was measured to be ~ 3 nm using Image J software. This result is in agreement with the crystal structure obtained previously. This value corresponds to the interdigitized hydrophobic layer distance indicating that the PDP units are responsible for the formation of thin hydrophobic walls of the vesicles. [27] Hence, it can be concluded that the

hydrophobic unit played a crucial role in the self assembly of the DEX-PDP-x derivatives into vesicular scaffolds.

AFM imaging was done to obtain topographical information and cross-sectional analysis of DEX-PDP derivatives. The average height of the vesicles (about 8 nm) is much smaller than their average diameter (about 200 nm). This may be due to two reasons. First, the height measured with tapping mode AFM may be lower than the real height due to deformation of the vesicle surface by the AFM tip. Second, this result can be attributed to vesicle collapse during the drying process. As shown in the phase image (See Figure 3.10) the center part and the edge of the vesicles respond differently to the AFM tip. This implies that the vesicles are hollow spheres and are filled with enough water under aqueous condition, and they become collapsed because of the escape of the water inside during the AFM sample preparation. [28]

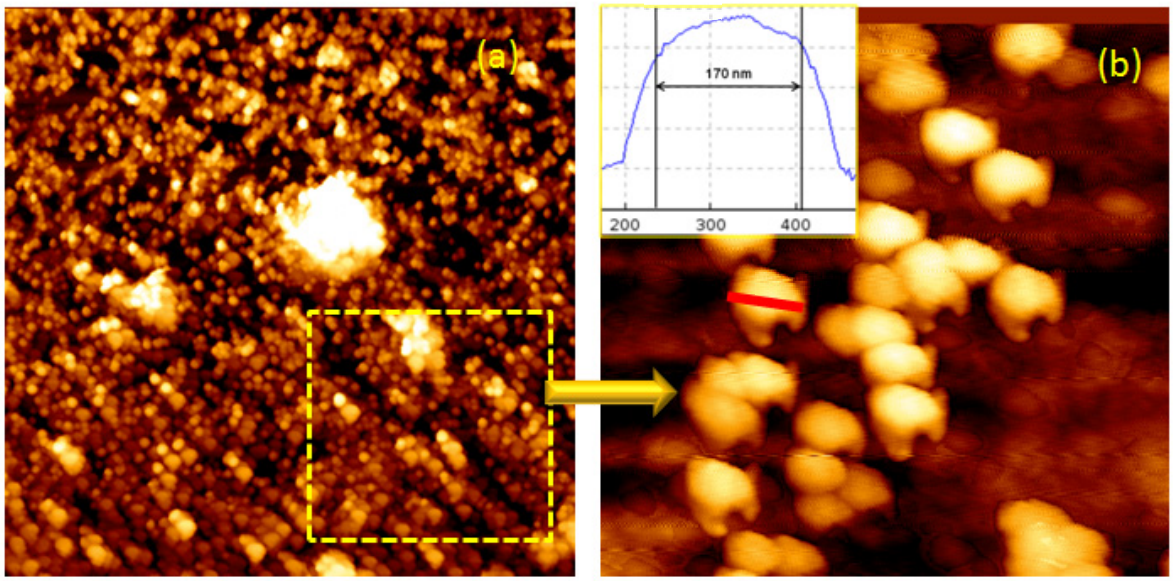

FIGURE 3.10 show the AFM phase image of DEX-PDP-7 and the enlarged image

DETERMINATION OF CRITICAL VESICULAR CONCENTRATION:

Above the critical association concentration (CAC) for the polymer, individual amphiphiles self-assemble to form nanostructures. The critical vesicular concentration was determined using pyrene as the fluorescent probe. The localization of pyrene in the hydrophobic layer of the vesicles gives an outlook into the characteristics of vesicle formation in water and its encapsulation resembles the

loading of hydrophobic drugs. Pyrene is extensively studied owing to its interesting photo physical properties, high quantum yield of fluorescence and its ability to form excimers. It shows vibronic bands (fine structure) in its monomer fluorescence spectra in water and its fine structure is sensitive to the solvent environment. The ratio of the first vibrational band (372 nm, I_1), the highest energy vibrational band, to the fluorescence intensity of the third vibrational band (385 nm, I_3) has been shown to correlate with solvent polarity. For example, in hydrocarbon solvent it is 0.6 and in water it is around 1.6. [29]

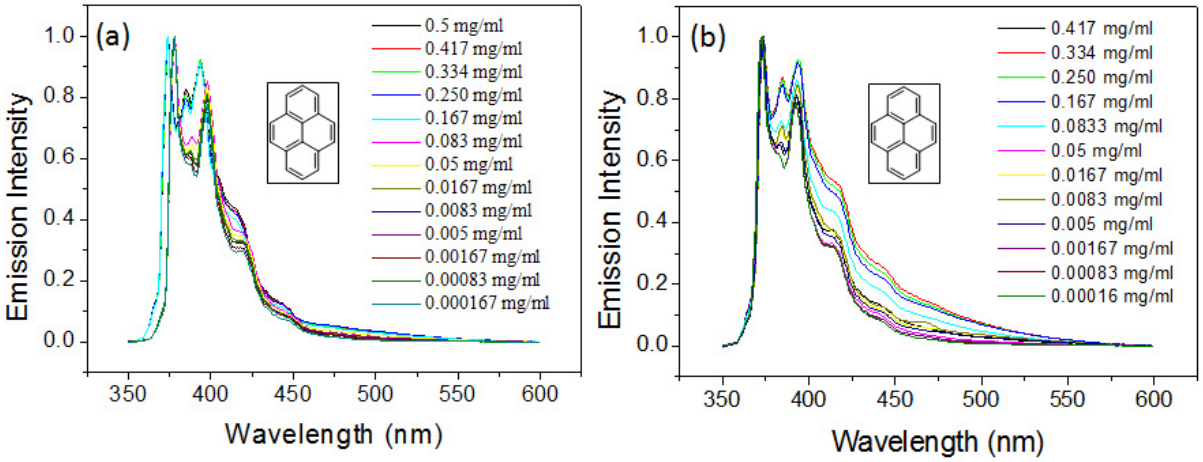

FIGURE 3.11 shows the emission spectrum of DEX-PDP-7 and DEX-PDP-13

Below the CVC, the I_1/I_3 ratio corresponds to a polar microenvironment. As the polymer concentration increases, the ratio decreases rapidly as a consequence of the more hydrophobic environment of pyrene. Above the CVC the I_1/I_3 ratio reaches a constant value due to the incorporation of pyrene into the hydrophobic region of the vesicle. The concentration of Pyrene was fixed to be 0.6 µM so as to prevent excimer formation and polymer concentration varied. At higher polymer concentration, i.e. above CVC, pyrene will prefer to stay in the hydrophobic layer of the vesicle. The emission spectra of DEX-PDP-7 and 13 are shown in Figure 3.11 .A plot of I_1/I_3 ratio was plotted against the log of concentration resulted in a sigmoidal curve. Here, we have chosen the onset of the slope since that indicates the onset of the association event. The critical vesicular concentration (CVC) for DEX-PDP-7 was found to be 7.2 $x10^{-4}$ M for DEX-PDP-7 and 3.04 $x10^{-4}$ M for DEX-PDP-13. The I_1/I_3 ratio obtained was in the range of $1< I_1/I_3<1.5$ which further confirms the localization of pyrene in the hydrophobic layer of the vesicles. [30] It must however be pointed out that the critical vesicular concentrations could not be determined for higher

substitutions of DEX-PDP derivatives owing to their insolubility in PBS buffer. Hence, this experiment was performed only for DEX-PDP-7, 13 and 25.

The emission spectrum for DEX-PDP-13 showed a hump at 445 nm due to the formation of a static excimer. [31] The CVC values obtained by fluorescence measurements confirm that the alkyl chain from the PDP unit governs the propensity of these molecules to self-assemble in water. The CVC was higher for lower substitution (DEX-PDP-7) in contrast to that for higher substitution (DEX-PDP-13). (See figure 3.12 b)

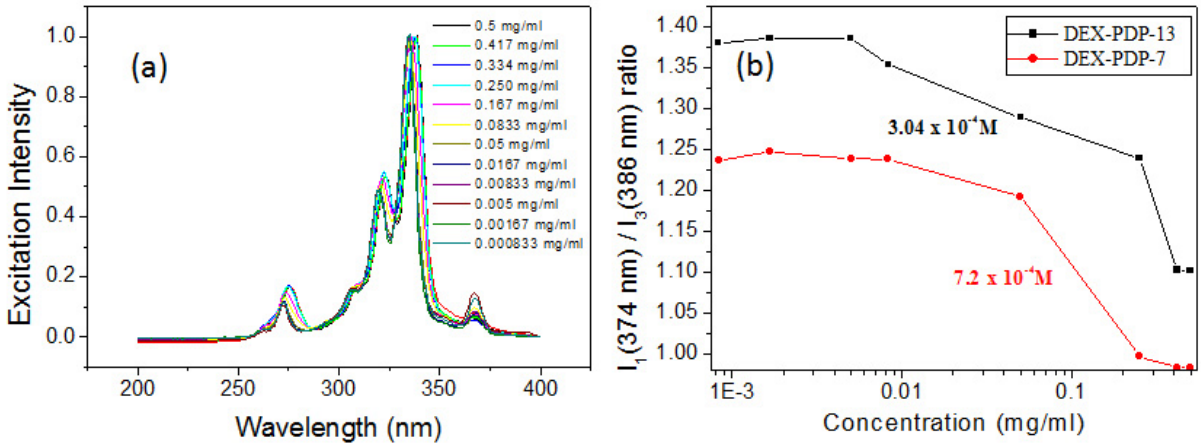

FIGURE 3.12 shows the excitation spectrum of DEX-PDP-7 and the CVC values for DEX-PDP-7 and DEX-PDP-13

Excitation spectra collected at both monomer and excimer emission of pyrene shows two peaks at 334 and 338 nm that are characteristic of pyrene monomer absorption in the hydrophilic and hydrophobic environment. (See figure 3.12 a)The excitation spectra were found to shift to a longer wavelength with an increase in the concentration of the polymer. This indicates the localization of pyrene in the hydrophobic domain of the self-assembled structures. Some bands in the 450 nm region appear for DEX-PDP-13 indicating the presence of pyrene excimers. [32]

A table showing different substitution along with their DLS size distributions and CVCs is given below. (See table 3.2).

SAMPLE NAME	DEGREE OFSUBSTITUTION (from NMR in %)	SIZE(from DLS in nm)	CVC (mg/ml)
DEX-PDP-7	7	160	8.33×10^{-3}
DEX-PDP-13	13	186	5×10^{-3}
DEX-PDP-25	25	570	5×10^{-3}
DEX-PDP-50	50	360	------

TABLE 3.2: summarizes the dependence of DLS sizes and CVC values on the degree of substitution

3.3. ENCAPSULATION OF HYDROPHILIC DYE MOLECULES

Rhodamine-B, a fluorescent dye with high quantum yield, photostability and red-emission was chosen as the probe to gain more insight into the interior of vesicles. It was hypothesised that owing to its hydrophilic nature, Rhodamine-B should be localized in the internal hollow cavity of the vesicles. The ability of the scaffold to stabilize the dye was tested by extensively dialyzing a solution containing the polymer and Rh-B against water. The unencapsulated Rh-B was removed by this process. The resulting Rh-B loaded solution was further dialyzed up to 7 days to ensure the stability of the loaded vesicles. The same experiment was carried out by using dextrin instead of DEX-PDP-7. As can be expected, dextrin did not stabilize Rh-B since there is no vesicle formation or self-assembly in case of dextrin alone.

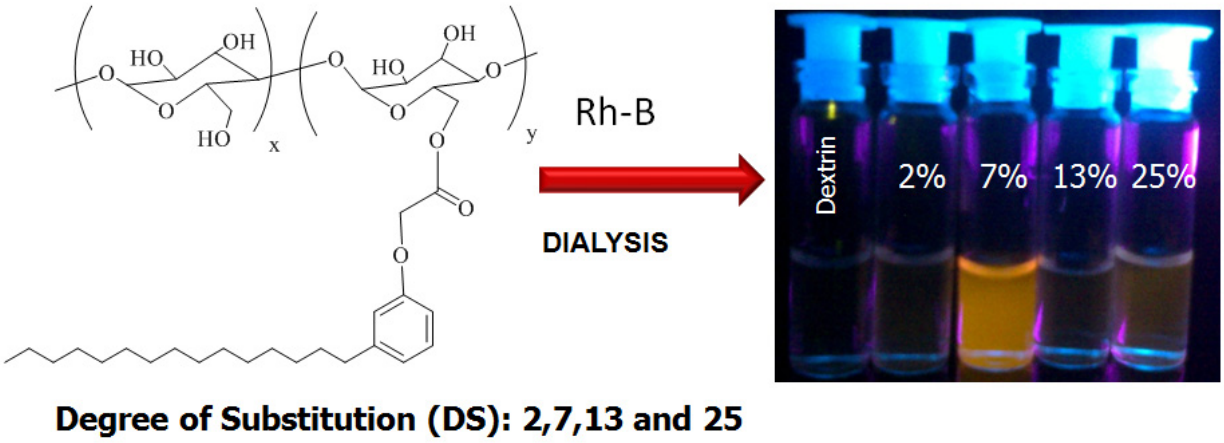

FIGURE 3.13 show the colour of Rh-B encapsulated scaffolds upon photo excitation. The number on the vials indicates the degree of substitution.

This experiment confirms the formation of vesicular scaffolds since micelles or nanoparticles cannot stabilize Rh-B in the hydrophobic core. [33]

Rh-B loaded scaffolds were characterized by DLS and TEM techniques. TEM

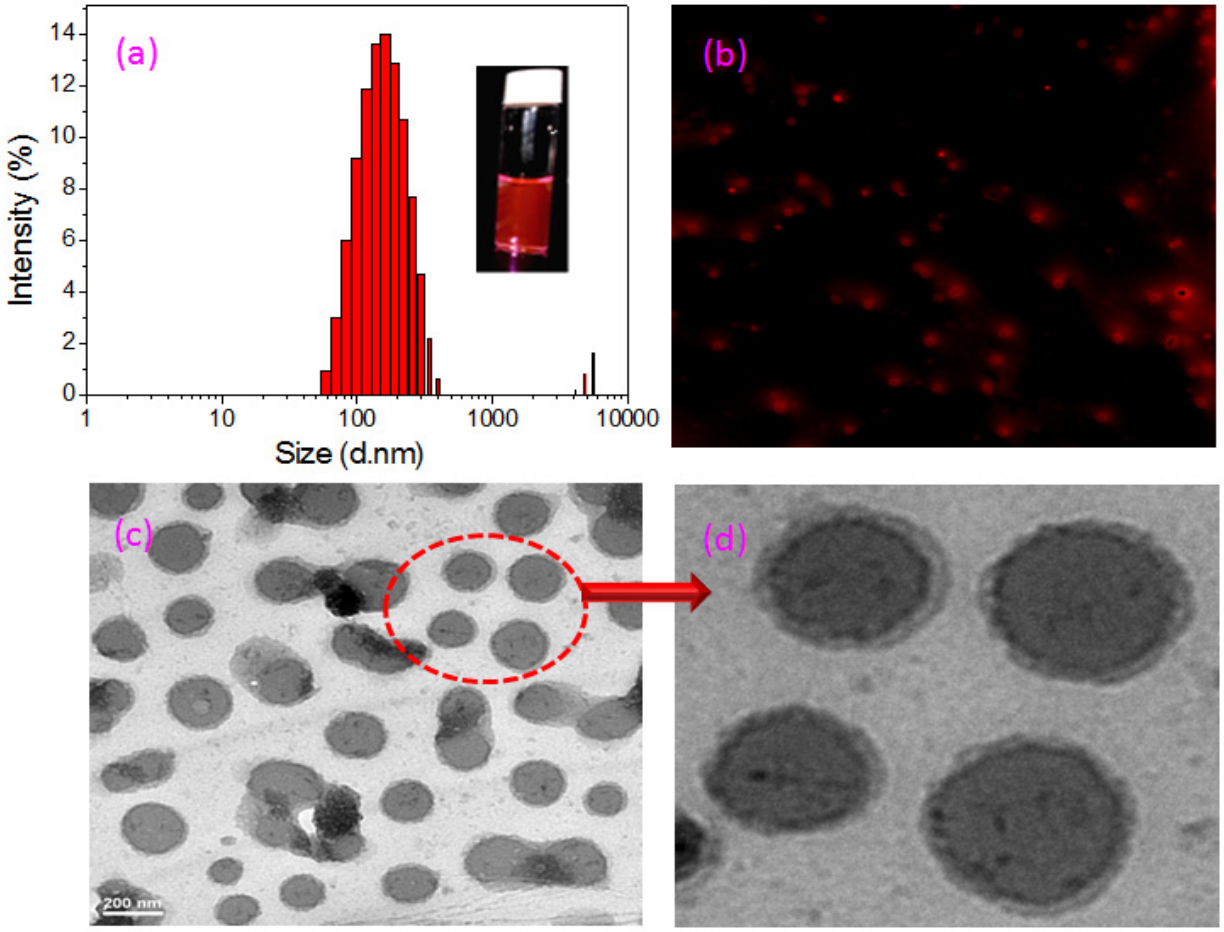

FIGURE 3.14 shows the (a) DLS profile, (b)) Fluorescence microscopy and (c) & (d)TEM images of DEX-PDP-7

images confirmed spherical assemblies with a dark outer ring but an absent hollow lumen [34] (3.14 c). This indicates the encapsulation of the dye in the interior. DLS measurements indicate that there is no appreciable size change after Rh-B encapsulation (3.14 b). Dye encapsulation was further confirmed by fluorescence microscopy where fluorescent dots in a dark background were observed with the fluorescence emanating from encapsulated Rh-B. (See Figure 3.14 d) It must however be pointed out that although DEX-PDP-7 could stabilize Rh-B effectively, the other substitutions could not stabilize Rh-B as effectively as DEX-PDP-7. The reasons for this could be twofold. It is possible that the packing achieved in case of higher substitutions is loose and hence Rh-B oozes out upon consistent perturbation

in the form of stirring during dialysis. It is also possible that there is some sort of change in the morphology of the self-assembled structure upon changing the substitution i.e. from vesicles to nanoparticles or micelles

3.4. *IN VITRO* RELEASE STUDIES

By modelling Rhodamine-B as a hydrophilic drug, the release kinetics was studied at physiological conditions. Figure 3.15 shows the *in-vitro* release characteristics of Rh-B encapsulated within DEX-PDP-7 vesicles. The amount of encapsulated Rh-B was determined using the equation:

DLC (%) = { Weight of drug in vesicles / Weight of Drug loaded vesicles} x 100

The encapsulation efficiency was calculated to be 0.1 wt. %.It can be concluded that Rh-B was released in a controlled manner. The plot shows sustained release of Rh-B with only 51% release in 24 hrs. (See figure 3.15 a) The DEX-PDP derivatives are linked by means of a simple ester linkage that can be readily cleaved in the presence of an enzyme, esterase. It has been reported that esterases are abundant in the cytoplasm of cells and that its concentration in liver microsomes is of

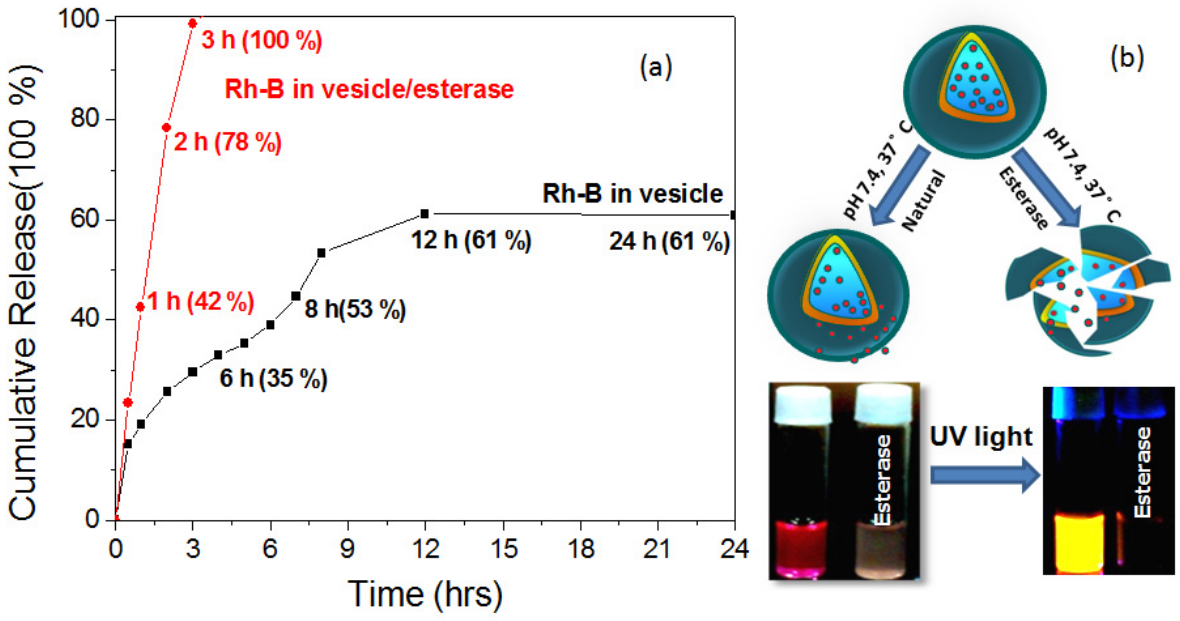

FIGURE 3.15: shows the (a) in vitro release profiles of Rh-B loaded DEX-PDP-7 and their show the colour of esterase treated solution upon photo excitation

the order of 9.8-30.5 U. According to a recent literature report, 10 U of esterase is the minimum amount required to cleave polysaccharide derivatives. [35]

Keeping this in mind, the release studies were carried out by adding 10 U horse liver esterase to the dialysis bag and the release kinetics were monitored thereafter. It was found that 100 % Rh-B release in over a period of 2 hrs.

This indicates that the ester linkage cleaves almost immediately upon action of esterase. As a consequence, the vesicular structure ruptures and releases Rh-B that accounts for the fast release of the dye. The same conclusion can be drawn by observing the solution in the dialysis bag prior in-vitro release and after subjecting it to esterase study. The solution shows precipitation owing to the rupture of the vesicular membrane. However, there was no precipitation in the absence of esterase. This indicates that the release in the absence of esterase is due to the natural leaching out due to constant perturbation in the form of stirring during dialysis, a hallmark of physical encapsulation since the release rate is governed by diffusion. But, in the presence of esterase, the release is due to the cleavage of the vesicle membrane by the action of esterase. Photographs taken after esterase study show precipitation and when held under UV light, does not show any orange emission indicating that no Rh-B is present. (See figure 3.15 b)This proves that the disruption of the vesicular scaffold is imperative for the release of the drug, in this case, Rh-B that has been chosen as the model hydrophilic drug. Moreover, studies are underway to ascertain the release kinetics for the choice of anti-cancer drugs that are hydrophobic as in case of Campothecin.

CONCLUSION

In this study, we have designed and synthesized starch based dextrin amphiphiles and used it for the loading and delivery of hydrophilic dye molecules. The novelties in the present strategy can be summed up as follows:

The approach uses biodegradable and renewable sources, dextrin and 3-pentadecyl phenol as starting materials, thus, advocating the ‘Green Chemistry’ approach. The amphiphiles were synthesized by grafting the hydrophobic unit on the dextrin backbone using DCC/DMAP coupling reaction and with varying degree of substitutions (DS). The structure of the newly synthesized DEX-PDP amphiphiles was confirmed by spectroscopic techniques like NMR, FT-IR. DEX-PDP amphiphiles self assembled under physiological conditions to form vesicles with sizes ranging from 160-500 nm depending on the DS. The vesicular assembly was further confirmed using SEM, HR-TEM, AFM and dynamic light scattering techniques. The vesicles were found to stabilize hydrophilic dye molecules (Rh-B and fluorescein) in their hydrophilic lumen. By modelling Rh-B as a hydrophilic drug, the in vitro release characteristics of Rh-B encapsulated within DEX-PDP-7 vesicles was studied under physiological conditions. The hydrophilic and hydrophobic segments in dextrin vesicles were stitched by means of an aliphatic ester-linkage. This was cleaved using an external stimuli i.e. esterase enzyme for the immediate release of the encapsulated Rh-B.

REFERENCES

1. Broz, P. *Polymer-based nanostructures for medical applications*, RSC Nanoscience and Nanotechnology (1st ed), **2008**, pp 3.
2. Shen, Y.; Jin, E.; Zhang. B.; Murphy, C.J.; Sui, M.; Zhao,J.; Wang,J.; Tang, J.; Fan,M.; Kirk, E.V.; Murdoch, W.J.; *J. Am. Chem. Soc.,* **2010**, *132*, 4259-4265.
3. Farokhzad, O.C.; Langer, R, *ACS Nano* **2009**, *3*, 160.
4. Uhrich, K.E.; Canizzaro S.M.; Langer,R.; Shakesheff, K.M. *Chem. Rev*., **1999**, *99*, 3181.
5. Ambade, A.V.; Savariar, E.N.; Thayumanavan, S. *Mol. Pharm*. **2005**, *2*, 264.
6. Whitesides, G.M.; Mathias, J.P.; Seto, C.T. *Science* **1991**, *254*, 1312.
7. Torchilin, V.P *J. Controlled Release* **2001**, *73*, 137.
8. (a) Maeda, H.; Seymour, L. W.; Miyamoto, Y. *Bioconjugate Chem.* **1992**, *3*, 351 (b)Seymour, L. W., Miyamoto, Y., Maeda, H., Brereton, B. M., Strohalm, J., Ulbrich, K., and Duncan, R. *Eur. J. Cancer.* **1995**, *31A*, 766 (c) Takakura, Y., and Hashida, M. *Crit. Rev. Oncol. Hematol.* **1995**, *18*, 207-231 (d) Maeda, H., Wu, J., Sawa, T., Matsumura, Y., and Hori, K *J. Controlled Release* **2000**, *65*, 271-284.
9. Gamblin, D.P.; Scanlan, E.M.; Davis, B.G., *Chem. Rev.* **2009,***109*,131.
10. Hollingsworth, R.I.; Wang,G.; *Chem Rev*. **2000**, 4267.
11. Dwek, R.A.; *Chem. Rev.* **1996**, *96*, 683.
12. Lehninger, *Principles of Biochemistry (4 th edition),* **2004**, pp 238-253.
13. (a) Tomasik, P., & Schilling, Ch. H. (2004). Chemical modification of starch. *Advances in Carbohydrate Chemistry and Biochemistry*, **59**,176–404(b) Angellier, H., Molina-Boisseau, S., Belgacem, M. N., & Dufresne, A., *Langmuir* **2005**, *21*, 2425–2435.
14. (a) Wesslen, K.B.; Wesslen, B. *Carbo. Poly.* **2002**, *47*, 303 (b) Bargley, E. B.; Fanta, G. F.; Burr, R. C.; Doane, W. M.; Russell, C. R. *Polym. Eng. Sci.* **1977**, *17*, 311.
15. Bian, F.; Jia,l.; Yu,W.; Liu,M. Carbo. Poly. **2009**, *76*, 454.
16. Hreczuk-Hirst,D.; Chicco, D.; German,L.; Duncan R.; *International Journal of Pharmaceutics*, **2001**, *230*, 57-66.
17. Hreczuk-Hirst,D.; Chicco, D.; German,L.; Duncan R.; *Journal of Bioactive and Compatible polymers*, **2001** ,*16*,353-365.
18. Carvalho, J.M.; Coimbra, M.A.; Gama, F.M. *Carbo. Poly*. **2009**, *75*, 322.

19. Hardwicke,J.; Moseley,R.; Stephens,P.; Harding, K.; Duncan,R.; Thomas, D.W. *Mol. Pharm*. **2010**, *7*, 699.
20. (a) Duncan, R.; Gilbert,H.R.P.; Carbajo, R.J.; Vicent, M.J. *Biomacromolecules*, **2008**, *9*, 1146 (b)Ferguson, E.L.; Duncan, R. *Biomacromolecules*, **2009**, *10*, 1358.
21. Senanayake, T.H.; Warren, G.; Vinogradov, S.V. *Bioconjugate Chemistry*, **2011**, *22*, 1983.
22. (a) Gonçalves, C.; Martins, J.A.; Gama, F.M.; *Biomacromolecules*, **2007**, *8*,392-398 (b) Gonçalves, C.; Periera,P.; Schellenberg,P.; Coutinho, P.J.; Gama, F.M. *Journal of Biotechnology and Nanobiotechnology*, **2012**, *3*, 178.
23. Molinos, M.; Carvalho,V.; Silva, D.M.; Gama, F.M. *Biomacromolecules*, **2012**, *13*, 517.
24. (a) Chakraborty, S.; Sahoo,B.; Teraoka, I.; Miller, L.M.; Gross, R.A. *Macromolecules*, **2005**, *38*,61(b)Choi, E.J.; Kim, C.H.; Park, J.K. *Macromolecules*, **1999**, *32*, 7402.
25. Ferreira, S.A.; Coutinho, P.J.G.; Gama, F.M. *Langmuir*, **2010,** *26*, 11413.
26. (a) Bachelder, E. M.; Beaudette, T. T.; Broaders, K. E.; Dashe, J.; Frechet, J. M. J. *J.Am. Chem. Soc.* **2008**, *130*, 10494-10495. (b) Broaders, K. E.; Cohen, J. A.; Beaudette, T. T.; Bachelder, E. M.; Frechet, J. M. J. *PNAS* **2009**, *106*, 5497. (c) Keliher, E. J.; Yoo, J.; Nahrendorf, M.; Lewis, J. S.; Marinelli, B.; Newton, A.; PittetM. J.; Weissleder, R. *Bioconjugate Chem.* **2011**, *22*, 2383-2389.
27. Pramod,P.S.; Takamura,K.; Chaphekar,S; Balasubramanian,N.; Jayakannan,M.; *Biomacromolecules*, **2012**, *13*, 3627-3640.
28. (a) Yang, M.; Wang, W.; Yuan, F.; Zhang, X.; Li, J.; Liang, F.; He, B.; Minch, B.; Wegner, G,; *J. Am. Chem. Soc.* **2005**, *127*, 15107-15111. (b) Tanaka,Y.; Miyachi,M.; Kobuke, Y. *Angew. Chem. Int. Ed*. **1999**, *4*, 38.
29. (a)Winnik, F.M. *Chem. Rev.* **1993**, *93*, 587 (b)Baig.C.k.; Duhamel,J.; Fung,S.Y.; Bezaire,J.; Chen,P. *J. Am. Chem. Soc.* **2004**,*126*,7522.(c)Kalyanasundaram,K.; Thomas,J.K., *J. Am. Chem. Soc.,* **1977**, *99*, 2039 (d)Kawaguchi,S.;Yekta,A.;Duhamel,J.; Winnik,M.A. *J.Phys. Chem.* **1994**,*98*,7891(e) Kawaguchi,S.;Yekta,A.;Duhamel,J.; Winnik,M.A. *J.Phys. Chem.* **1993**, *97*,2759.

30. (a)Changez, Kang, M.G.N.; Lee, C.H.; Lee, J.S. *Small*, **2010**,*6*,638(b)De Maria, P.; Fontana,A.; Saini, G.; D'Aurizio,E.; Cerichelli,G.; Chiarini,M.;Angelini,G.; Gasbarri,C. *Colloids Surf.B* **2011** *87*,73.(b) Delample,M.; Jerome,F.;Barrault,J.; Douliez, J.P. *Green Chem*. **2011**, *13*, 64.
31. (a)Dong, D.C.; Winnik, M.A. *Photochem. Photobiol*. **1982**, *35*, 17(b) Dong, D.C.; Winnik, M.A. *Can. J. Chem* **1984**, *62*, 2560.
32. Kashyap, S.; Jayakannan, M. *J. Phys. Chem. B* **2012**, *116*, 9820.
33. (a)Yan, Q.; Yuan, J.; Cai, Z.; Xin, Y.; Kang, Y.; Yin, Y.; *J. Am. Chem. Soc.* **2010**, *132*, 9268-9270. Yan, Q.; Zhou, R.; Fu, C.; Zhang, H.; Yin, Y.; Yuan, J.; *Angew. Chem.. Int. Ed.* **2011**, *50*, 4923-4927. (b) Xu, J.; Tao, l.; Boyer, C.; Lowe, A. B.; Davis, T.; *Macromolecules*, **2011**, *44*, 299-312. (c) Koley, P.; Pramnanik, A.; *Soft Matter*, **2012**, *8*, 5364-5374. (d) Du, J.; Armes, S. P.; *J. Am. Chem. Soc.* **2005**, *127*, 12800-12801.
34. Du.J.; Armes, S.P. *Langmuir* **2009**, *25*, 9564.
35. (a)Nunzio, M. R. D.; Cohen, B.; Douhal, A. *J. Phys. Chem. A*. **2011**, *115*, 5094-5104 (b) Alter,S. C.; Metcalfe, D. D.; Bradford, T. R.; Schwartz, L. B.*; Biochem. J.* **1987**, *248*, 821-827.

APPENDIX

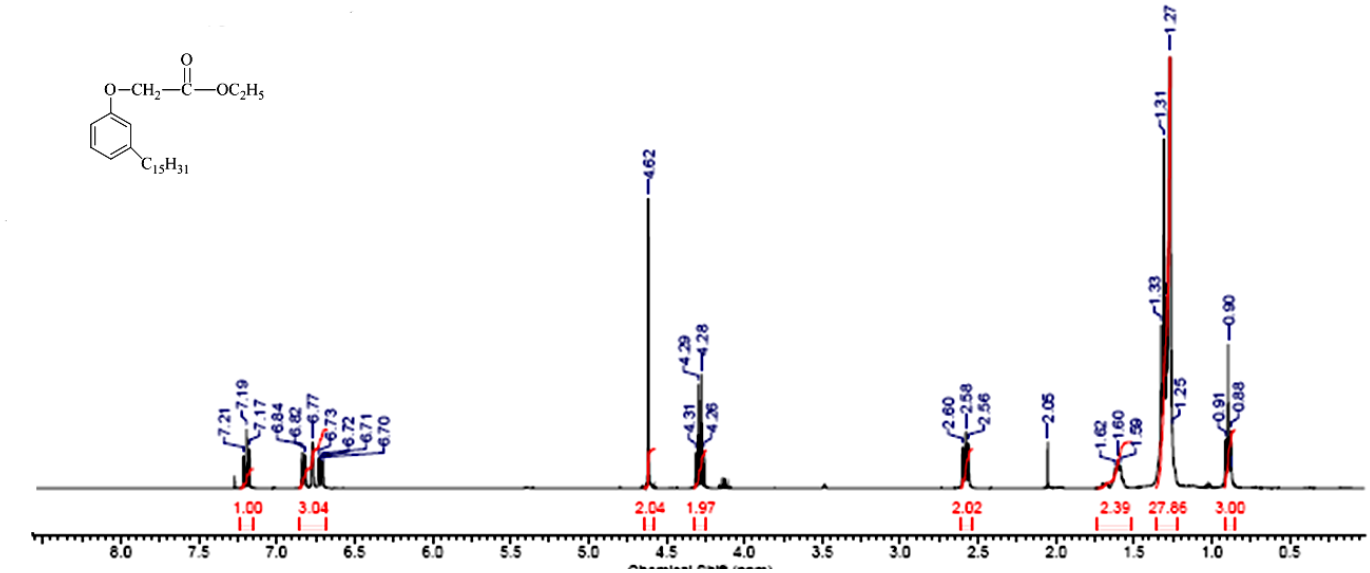
O
O–CH2–C–OC2H5
C15H31
7.21
7.19
7.17
6.84
6.82
6.77
6.73
6.72
6.71
6.70
4.62
4.29
4.28
4.31
4.26
2.60
2.58
2.56
2.05
1.62
1.60
1.59
1.31
1.27
1.25
1.33
0.91
0.90
0.88
1.00
3.04
2.04
1.97
2.02
2.39
27.85
3.00

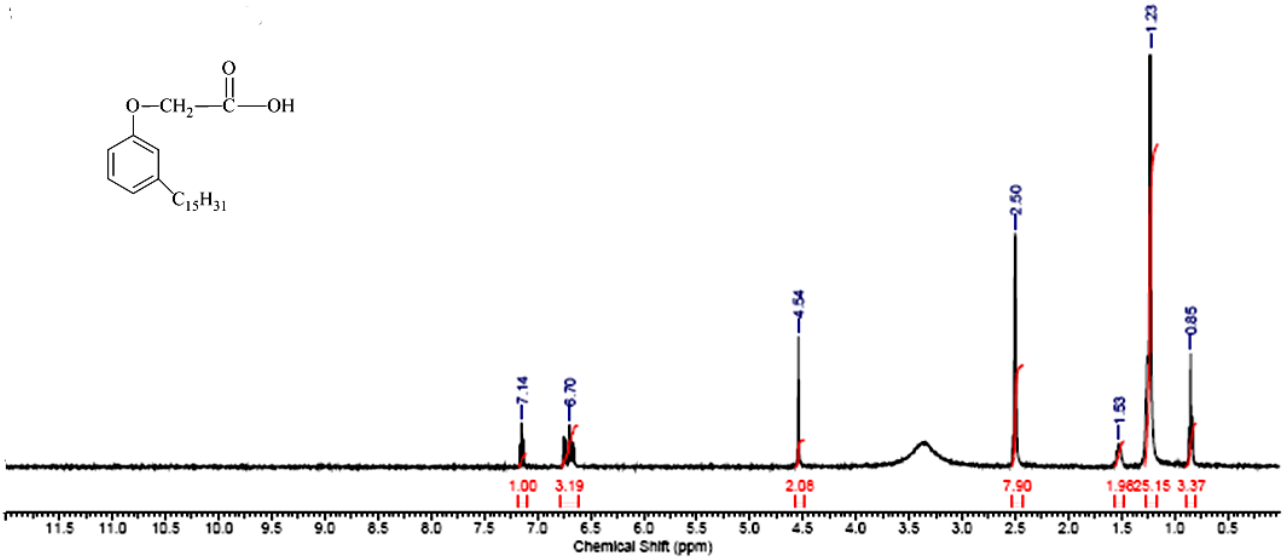
O
O–CH2–C–OH
C15H31
7.14
6.70
4.54
2.50
1.53
1.23
0.85
1.00
3.19
2.08
7.90
1.96
25.15
3.37
Chemical Shift (ppm)

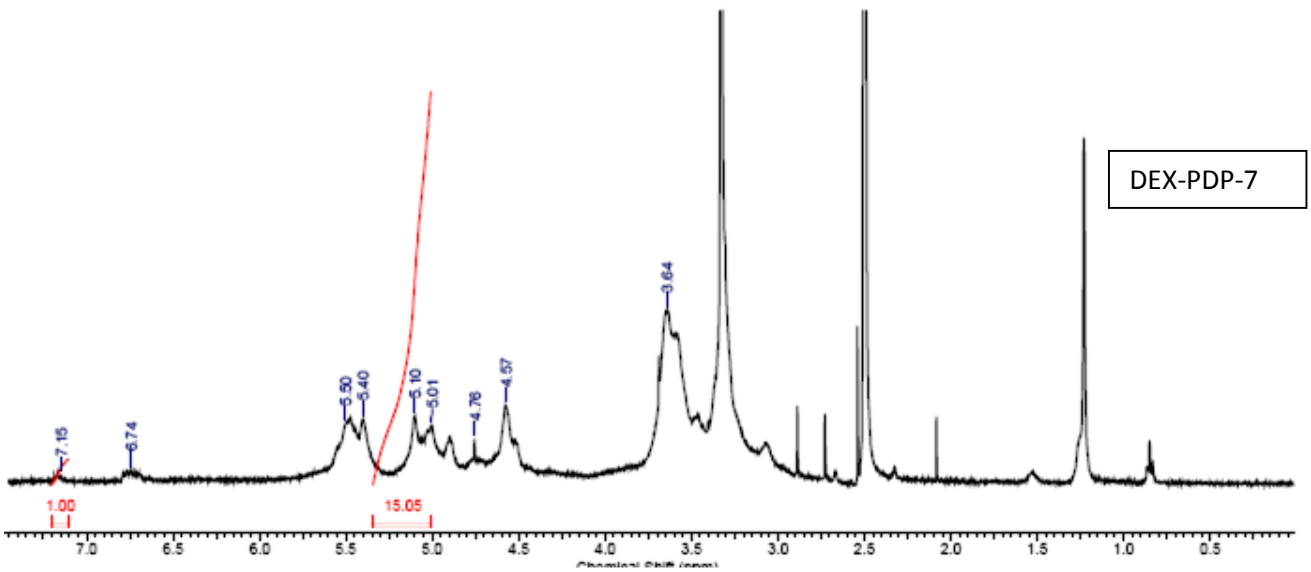
DEX-PDP-7
7.15
6.74
5.50
5.40
5.10
5.01
4.76
4.57
3.64
1.00
15.05

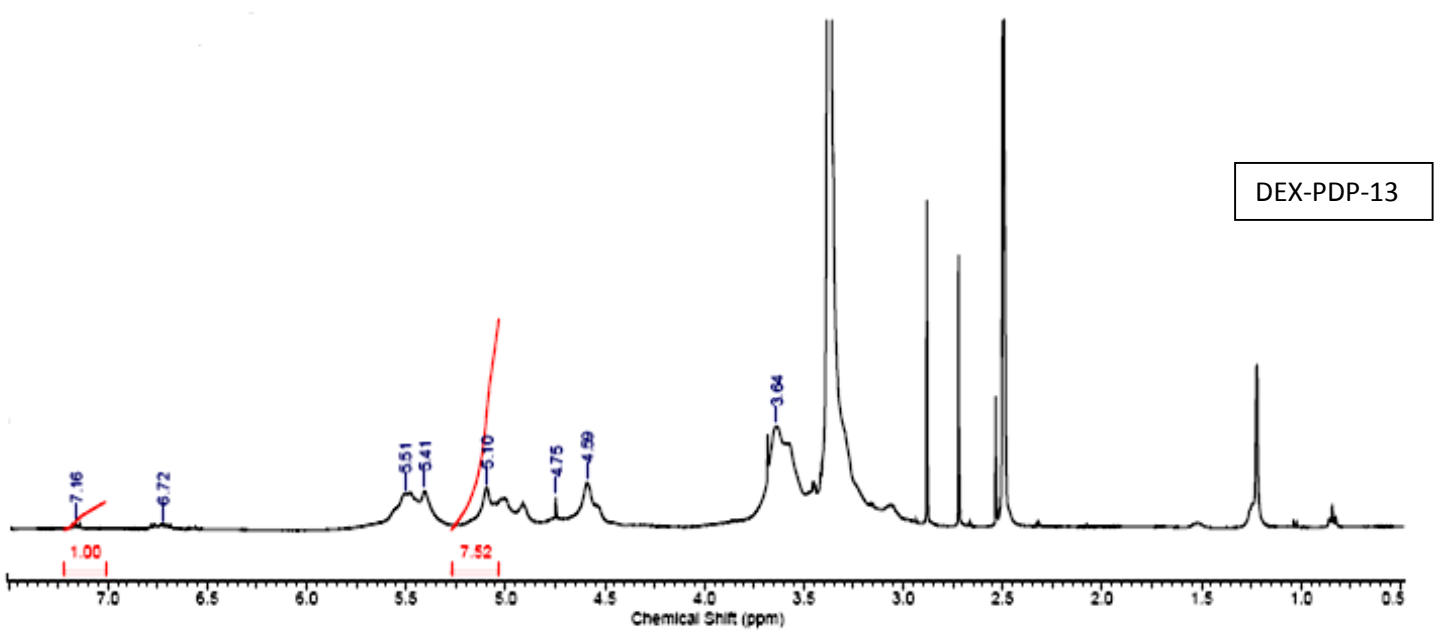
DEX-PDP-13
7.16
6.72
5.51
5.41
5.10
4.75
4.59
3.64
1.00
7.52
Chemical Shift (ppm)

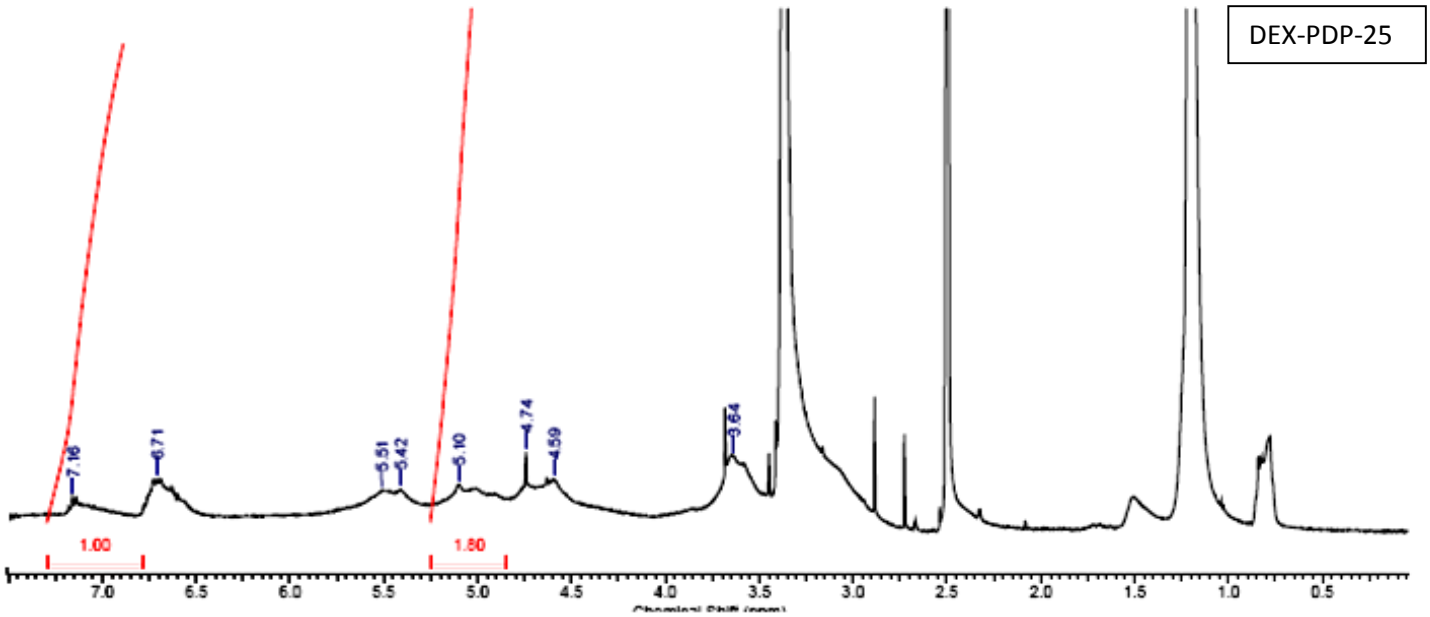
DEX-PDP-25
7.16
6.71
5.51
5.42
5.10
4.74
4.59
3.64
1.00
1.80

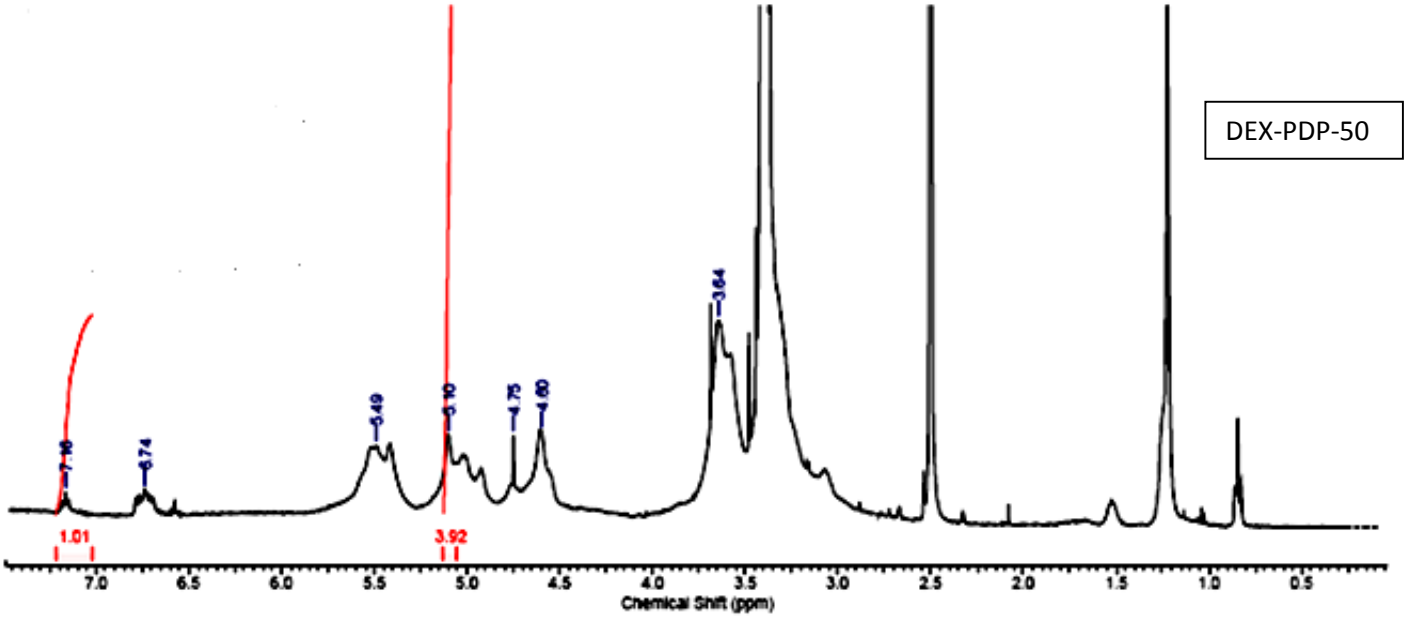
DEX-PDP-50
7.16
6.74
5.49
5.10
4.75
4.60
3.64
1.01
3.92
Chemical Shift (ppm)